Supplementary Information for the article

Diruthenium Complexes Having a Partially Hydrogenated Bipyridine Ligand: Plausible Mechanism for the Dehydrogenative Coupling of Pyridines at a Diruthenium Site

Toshiro Takao,* Takashi Kawashima, Ryo Nagae, Hideyuki Kanda, and Wataru Watanabe

Department of Chemical Science and Engineering, School of Materials and Chemical Technology, Tokyo Institute of Technology, 2-12-1 O-okayama, Meguro-ku, Tokyo 152-8552, Japan

Contents

1. Crystal data and results of XRD studies

Table S1. Crystallographic Data for **4a**, **5c**, **6b**, **7a**, and **8**.

	4a	**5c**	**6b**
(a) Crystal Data			
Empirical Formula	$C_{32}H_{46}N_2Ru_2$	$C_{36}H_{48}N_2O_4Ru_2$	$C_{37}H_{47}F_6N_3Ru_2$
Formula Weight	660.85	774.90	849.91
Crystal Description	Block	Prism	Block
Crystal Color	Red	Brown	Brown
Crystal size (mm)	0.12 × 0.08 × 0.06	0.31 × 0.28 × 0.22	0.38 × 0.31 × 0.26
Crystallizing Solution	Diethylether (2 °C)	Pentane (–20 °C)	Hexane (–30 °C)
Crystal System	Monoclinic	Orthorhombic	Triclinic
Space Group	*C*2/c (#15)	*Pnma* (#62)	*P-1* (#2)
a (Å)	19.7520(6)	16.0588(4)	10.3925(4)
b (Å)	8.49780(19)	19.8061(4)	11.2250(5)
c (Å)	34.8959(7)	10.6735(2)	17.5502(8)
α (°)			86.627(2)
β (°)	101.3836(8)		86.4350(10)
γ (°)			63.9190(10)
V (Å^3)	5742.0(2)	3394.84(12)	1834.17(14)
Z value	8	4	2
D_{calc} (g / cm^3)	1.529	1.516	1.539
Measurement Temp (°C)	–150	–150	–120
μ(MoKα) (mm^{-1})	1.075	0.930	0.884
(b) Intensity Measurements			
Diffractometer	RAXIS-RAPID	RAXIS-RAPID	RAXIS-RAPID
Radiation	MoKα	MoKα	MoKα
Monochromator	Graphite	Graphite	Graphite
2θmax	60 °	55 °	55°
Reflections Collected	31904	31156	18139
Independent reflections	8193 (R_{int} = 0.0290)	3969 (R_{int} = 0.0222)	8290 (R_{int} = 0.0367)
Reflections Observed (> 2σ)	7393	3752	7400
Abs. Correction type	Empirical	Empirical	Empirical
Abs. Transmission	0.8708 (min.) 1.0000 (max.)	0.8109 (min.), 1.0000 (max.)	0.6945 (min.), 1.0000 (max.)
(c) Refinement (SHELXL-2016/6)			
R_1 (I > 2σ(I))	0.0224	0.0228	0.0312
wR_2 (I > 2σ(I))	0.0486	0.0581	0.0779
R_1 (all data)	0.0268	0.0242	0.0356
wR_2 (all data)	0.0504	0.0589	0.0810
Data/Restraints/Parameters	8193 / 0 / 378	3969 / 0 / 246	8290 / 0 / 478
GOF	1.064	1.080	1.026
Largest diff. peak and hole (e.Å^{-3})	0.837 and –0.631	1.234 and –0.703	1.096 and –0.374
CCDC deposition number	1901042	1901043	1901044

Table S1. Crystallographic Data for **4a**, **5c**, **6b**, **7a**, and **8** (continued).

	7a	**8**
(a) Crystal Data		
Empirical Formula	$C_{32}H_{42}N_2Ru_2$	$C_{32}H_{40}N_2Ru_2$
Formula Weight	656.81	654.80
Crystal Description	Platelet	Platelet
Crystal Color	brown	black
Crystal size (mm)	0.15 × 0.15 × 0.03	0.10 × 0.05 × 0.02
Crystallizing Solution	Hexane (–30 °C)	Hexane (–30 °C)
Crystal System	Monoclinic	Triclinic
Space Group	*C*2/c (#15)	*P-1* (#2)
a (Å)	21.875(3)	10.8926(9)
b (Å)	17.503(2)	16.1224(14)
c (Å)	16.448(2)	16.4294(12)
α (°)		89.244(2)
β (°)	112.870(8)	78.917(2)
γ (°)		77.643(2)
V (Å^3)	5802.3(13)	2764.7(4)
Z value	8	4
D_{calc} (g / cm^3)	1.504	1.573
Measurement Temp (°C)	–150	–100
μ(MoKα) (mm^{-1})	1.063	1.116
(b) Intensity Measurements		
Diffractometer	RAXIS-RAPID	RAXIS-RAPID
Radiation	MoKα	MoKα
Monochromator	Graphite	Graphite
2θmax	55°	50°
Reflections Collected	26900	24144
Independent reflections	6557 (R_{int} = 0.1264)	10046 (R_{int} = 0.1091)
Reflections Observed (> 2σ)	3670	6214
Abs. Correction type	Numerical	Empirical
Abs. Transmission	0.8647 (min.), 0.9402 (max.)	0.5300 (min.), 1.0000 (max.)
(c) Refinement (SHELXL-2016/6)		
R_1 (I > 2σ(I))	0.0537	0.0821
wR_2 (I > 2σ(I))	0.1018	0.1807
R_1 (all data)	0.1146	0.1312
wR_2 (all data)	0.1230	0.2146
Data/Restraints/Parameters	6557 / 0 / 337	10046 / 0 / 794
GOF	0.956	0.967
Largest diff. peak and hole (e.Å^{-3})	1.070 and –0.888	1.523 and –2.360
CCDC deposition number	1901045	1901046

(a) $(Cp^*Ru)_2\{\mu\text{-}\eta^2\text{-}4,4'\text{-}Me_2dhbpy\}(\mu\text{-}H)(H)$ (**4a**)

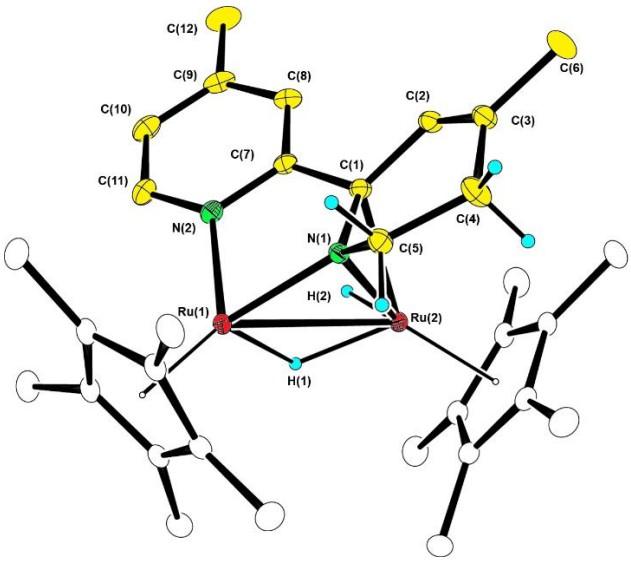

Figure S1. Molecular structure and labelling scheme of **4a** with thermal ellipsoids at a 40% probability. Selected bond lengths (Å) and angles (deg): Ru(1)–Ru(2) 2.89518(17), Ru(1)–N(1) 2.0552(13), Ru(1)–N(2) 2.1048(13), Ru(2)–N(1) 2.0934(13), Ru(2)–C(1) 2.1764(15), C(1)–C(2) 1.472(2), C(1)–C(7) 1.472(2), C(1)–N(1) 1.4168(19), C(2)–C(3) 1.338(2), C(3)–C(4) 1.496(2), C(4)–C(5) 1.509(2), C(5)–N(1) 1.463(2), C(7)–C(8) 1.404(2), C(7)–N(2) 1.363(2), C(8)–C(9) 1.384(2), C(9)–C(10) 1.401(3), C(10)–C(11) 1.378(2), C(11)–N(2) 1.351(2), N(1)–Ru(1)–N(2) 78.14(5), C(7)–C(1)–N(1) 113.80(13), C(1)–C(7)–N(2) 114.71(13), Ru(1)–N(1)–C(1) 114.13(10), Ru(1)–N(2)–C(7) 115.19(10).

(b) $(Cp^*Ru)_2\{\mu\text{-}\eta^4\text{-}4,4'\text{-}(COOEt)_2dhbpy\}$ (**5c**)

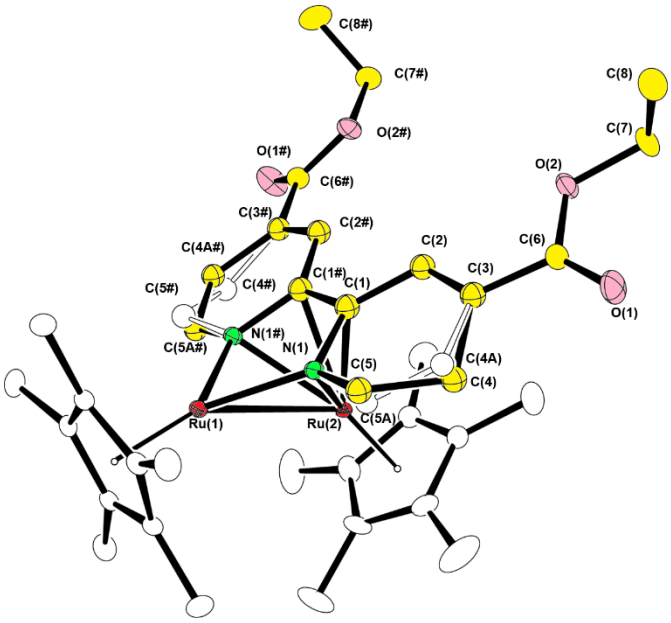

Figure S2. Molecular structure and labelling scheme of **5c** with thermal ellipsoids at a 30% probability. Selected bond lengths (Å) and angles (deg): Ru(1)–Ru(2) 2.9037(2), Ru(1)–N(1) 2.0584(13), Ru(2)–N(1) 2.2569(14), Ru(2)–C(1) 2.1805(16), C(1)–C(1#) 1.425(3), C(1)–C(2) 1.441(2), C(1)–N(1) 1.405(2), C(2)–C(3) 1.355(2), C(3)–C(4) 1.492(5), C(3)–C(4A) 1.459(4), C(4)–C(5) 1.504(6), C(4A)–C(5A) 1.373(6), C(5)–N(1) 1.468(5), C(5A)–N(1) 1.405(5), N(1)–Ru(1)–N(1A) 75.72(8), C(1#)–C(1)–N(1) 113.09(9), Ru(1)–N(1)–C(1) 118.15(11).

(c) $(Cp^*Ru)_2\{\mu\text{-}\eta^4\text{-}4,4'\text{-}(CF_3)_2dhbpy\}(^tBuNC)$ (**6b**)

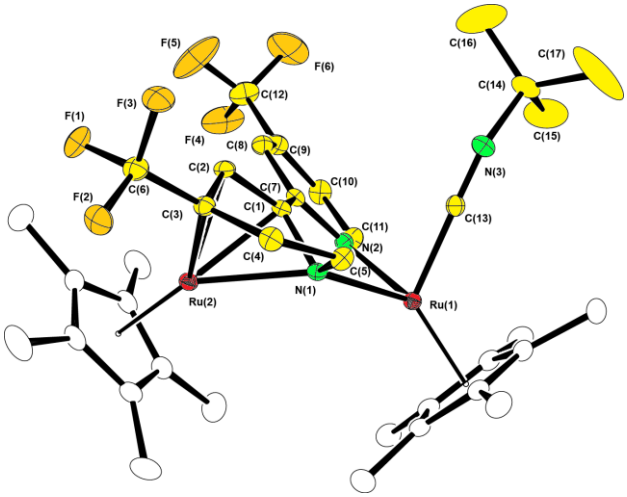

Figure S3. Molecular structure and labelling scheme of **6b** with thermal ellipsoids at a 30% probability. Selected bond lengths (Å) and angles (deg): Ru(1)···Ru(2) 4.126(3), Ru(1)–N(1) 2.1755(18), Ru(1)–N(2) 2.1145(18), Ru(1)–C(13) 1.904(2), Ru(2)–N(1) 2.2833(18), Ru(2)–C(1) 2.113(2), Ru(2)–C(2) 2.120(2), Ru(2)–C(3) 2.178(2), C(1)–N(1) 1.408(3), C(1)–C(2) 1.428(3), C(1)–C(7) 1.454(3), C(2)–C(3) 1.451(3), C(3)–C(4) 1.517(3), C(4)–C(5) 1.520(3), C(5)–N(1) 1.488(3), C(7)–N(2) 1.360(3), C(7)–C(8) 1.405(3), C(8)–C(9) 1.384(3), C(9)–C(10) 1.386(4), C(10)–C(11) 1.379(4), C(11)–N(2) 1.351(3), C(13)–N(3) 1.175(3), C(1)–N(1)–C(5) 112.89(17), C(2)–C(1)–N(1) 116.66(18), C(1)–C(2)–C(3) 113.72(19), C(2)–C(3)–C(4) 120.4(2), C(3)–C(4)–C(5) 108.76(18), C(4)–C(5)–N(1) 112.75(19), Ru(1)–C(13)–N(3) 176.9(2), C(13)–N(3)–C(14) 150.2(2).

(d) $(Cp^*Ru)_2(\mu\text{-}\eta^4\text{-}4,4'\text{-}Me2bpy)$ (**7a**)

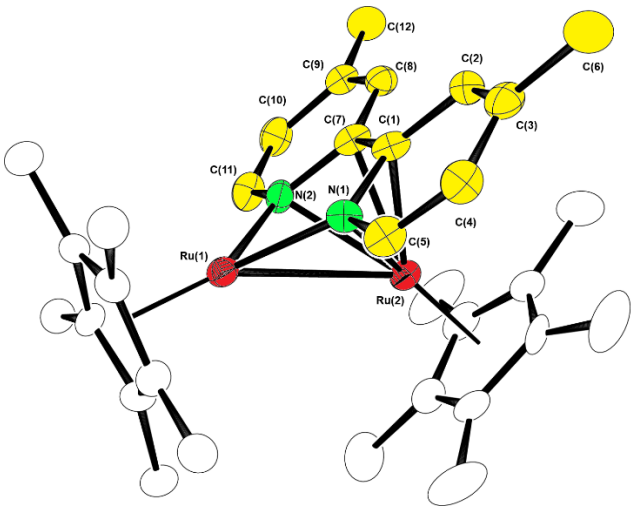

Figure S4. Molecular structure and labelling scheme of **7a** with thermal ellipsoids at a 40% probability. Selected bond lengths (Å) and angles (deg): Ru(1)–Ru(2) 2.9042(7), Ru(1)–N(1) 2.066(4), Ru(1)–N(2) 2.077(4), Ru(2)–N(1) 2.260(4), Ru(2)–N(2) 2.285(4), Ru(2)–C(1) 2.211(6), Ru(2)–C(7) 2.201(6), C(1)–C(7) 1.438(7), C(1)–C(2) 1.455(7), C(1)–N(1) 1.424(6), C(2)–C(3) 1.373(8), C(3)–C(4) 1.449(8), C(4)–C(5) 1.344(8), C(5)–N(1) 1.411(7), C(7)–C(8) 1.438(7), C(7)–N(2) 1.420(7), C(8)–C(9) 1.358(7), C(9)–C(10) 1.443(8), C(10)–C(11) 1.356(8), C(11)–N(2) 1.412(7), N(1)–Ru(1)–N(2) 75.35(17), Ru(1)–N(1)–C(1) 119.4(3), Ru(1)–N(2)–C(7) 118.6(3), N(1)–C(1)–C(7) 112.1(5), C(1)–C(7)–N(2) 113.2(4).

(e) $(Cp^*Ru)_2(\mu\text{-}\eta^2\text{-phen})(\mu\text{-H})(H)$ (**8**)

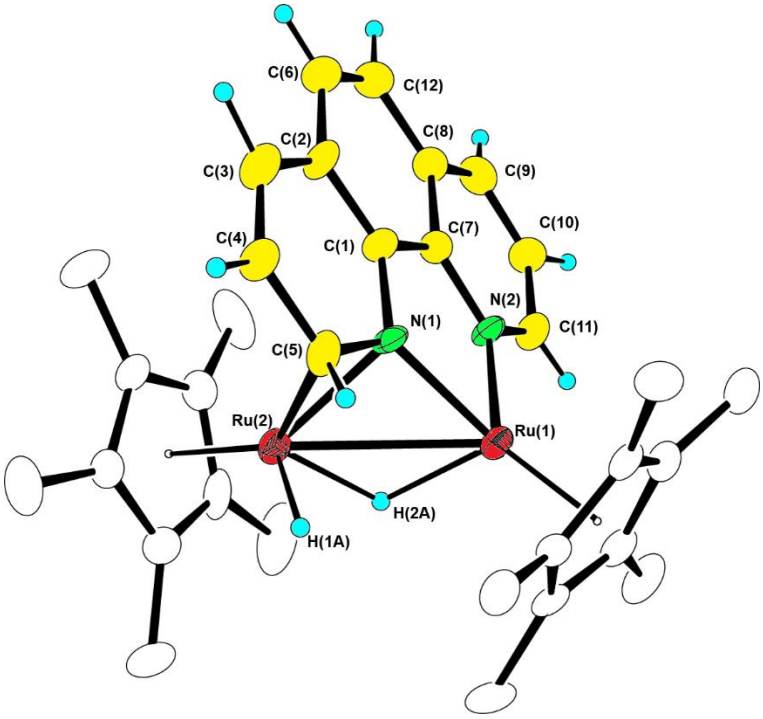

Figure S5. Molecular structure and labelling scheme of **8** with thermal ellipsoids at a 30% probability. Selected bond lengths (Å) and angles (deg): Ru(1)–Ru(2) 2.8776(9), Ru(1)–N(1) 2.053(7), Ru(1)–N(2) 2.092(7), Ru(2)–N(1) 2.101(8), Ru(2)–C(5) 2.195(10), C(1)−C(7) 1.440(13), C(1)–C(2) 1.373(14), C(1)–N(1) 1.412(12), C(2)–C(3) 1.439(14), C(3)–C(4) 1.342(16), C(4)–C(5) 1.449(15), C(5)–N(1) 1.413(11), C(7)–C(8) 1.419(13), C(7)–N(2) 1.353(12), C(8)–C(9) 1.395(15), C(9)–C(10) 1.356(16), C(10)–C(11) 1.397(15), C(11)−N(2) 1.351(12), N(1)–Ru(1)–N(2) 77.1(3), Ru(1)–N(1)–C(1) 116.8(6), Ru(1)–N(2)–C(7) 116.0(5), N(1)–C(1)–C(7) 112.7(8), C(1)–C(7)–N(2) 116.2(8).

2. Spectral data of the compounds

(a) $\{Cp^*Ru(\mu\text{-}4\text{-}MeC_5H_3N)(\mu\text{-}H)\}_2$ (**2a**)

^{1}H NMR (400 MHz, benzene-d_6, 25 °C): δ –9.33 (s, 2H, Ru*H*), 1.77 (s, 6H, C^4*Me*), 1.89 (s, 15H, Cp*), 2.09 (s, 15H, Cp*), 6.04 (d, *J* = 5.3 Hz, C^5*H*), 6.95 (s, C^3*H*), 8.00 ppm (d, *J* = 5.3 Hz, C^6*H*).

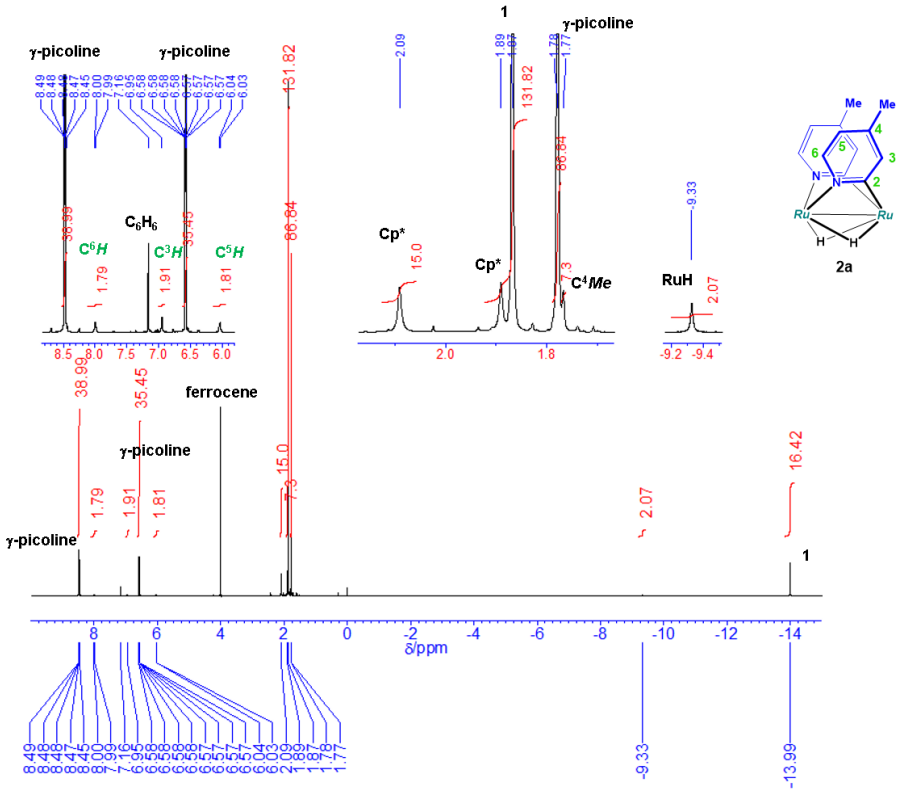

Figure S6. ^{1}H NMR spectrum of the mixture obtained by the reaction of **1** with γ-picoline at 25 °C; recorded after 5 min (400 MHz, C_6D_6, 25 °C).

(b) $(Cp^*Ru)_2\{\mu\text{-}\eta^2\text{-}4,4'\text{-}Me_2dhbpy\}(\mu\text{-}H)(H)$ (**4a**)

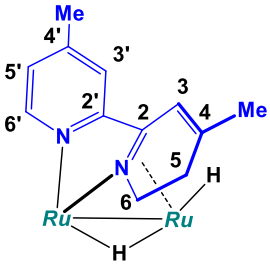

^{1}H NMR (400 MHz, Benzene-d_6, 25 ° C): δ –15.30 (d, J = 4.0 Hz, 1H, RuH), –11.56 (d, J = 4.0 Hz, 1H, RuH), 1.6* (m, 1H, C_5H_2), 1.65 (s, 3H, $C^{4'}Me$), 1.77 (s, 15H, C_5Me_5), 1.83 (s, 3H, C^4Me), 1.88 (s, 15H, C_5Me_5), 1.9* (m, 1H, C^5H_2), 3.84 (ddd, J = 13.2, 7.0, 3.5 Hz, 1H, C^6H_2), 4.52 (ddd, J = 13.2, 10.4, 5.6 Hz, 1H, C^6H_2), 5.90 (d, J = 6.0 Hz, 1H, $C^{5'}H$), 6.29 (s, 1H, C^3H), 6.62 (s, 1H, $C^{3'}H$), 7.92 ppm (d, J = 6.0 Hz, 1H, $C^{6'}H$). (* confirmed by H–H COSY). ^{13}C NMR (100 MHz, Benzene-d_6, 25 ° C): δ 11.4 (q, J_{CH} = 126 Hz, C_5Me_5), 12.0 (q, J_{CH} = 126 Hz, C_5Me_5), 20.8 (q, J_{CH} = 127 Hz, C^7Me), 24.0 (q, J_{CH} = 126 Hz, C^3Me), 29.9 (dd, J_{CH} = 130, 121 Hz, C^5), 59.3 (dd, J_{CH} = 138, 138 Hz, C^6), 62.7 (s, C^2), 79.6 (s, C_5Me_5), 93.9 (s, C_5Me_5), 114.6 (d, J_{CH} = 159 Hz, $C^{3'}$), 117.1 (d, J_{CH} = 161 Hz, $C^{5'}$), 122.9 (s, C^4), 123.6 (d, J_{CH} = 159 Hz, C^3), 141.4 (s, $C^{4'}$), 150.4 (d, J_{CH} = 175 Hz, $C^{6'}$), 173.4 ppm (s, $C^{2'}$). IR (KBr, cm^{-1}): 2974, 2945, 2893, 2852, 1986 (ν(RuH)), 1607, 1540, 1469, 1373, 1300, 1027, 1011, 795.

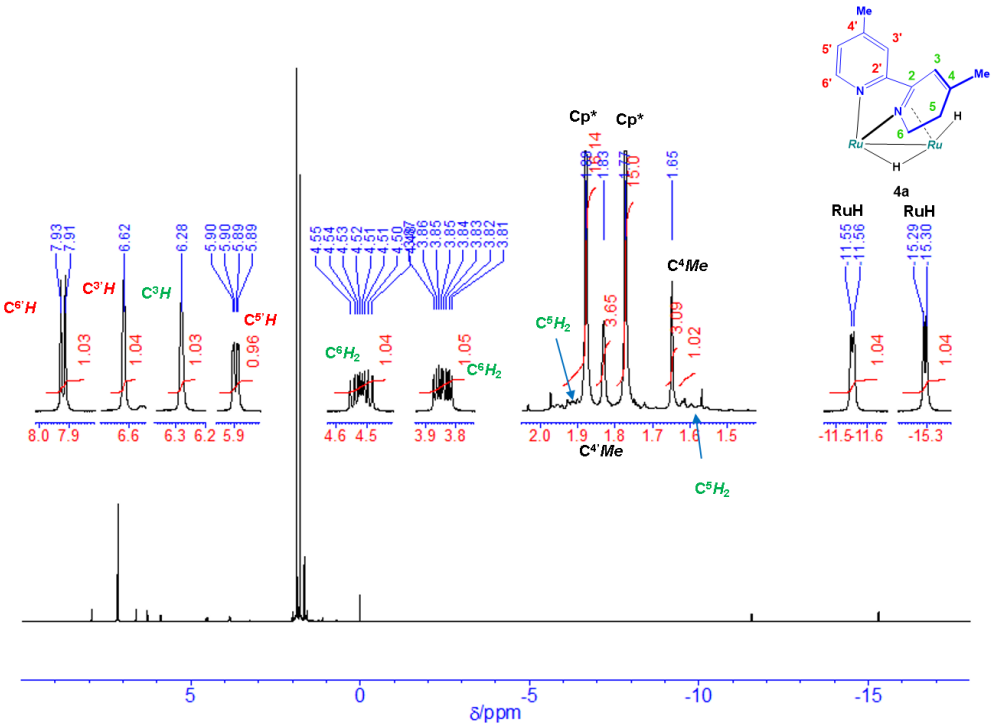

Figure S7. ^{1}H NMR spectrum of **4a** (400 MHz, C_6D_6, 25 °C).

Table S2. Coupling parameters for the methylene protons at the C^6 position of **4a**.

		δ /ppm	W /Hz	*J* [1]	*J* [2]	*J* [3]
1	C^5H^a	(1.601)*	1.40			
2	C^5H^b	(1.903)*	1.40	(16.40)		
3	C^6H^a	3.843	1.40	3.50	7.00	
4	C^6H^b	4.518	1.30	10.40	5.60	13.20

* obscured by the Cp* and Me signals

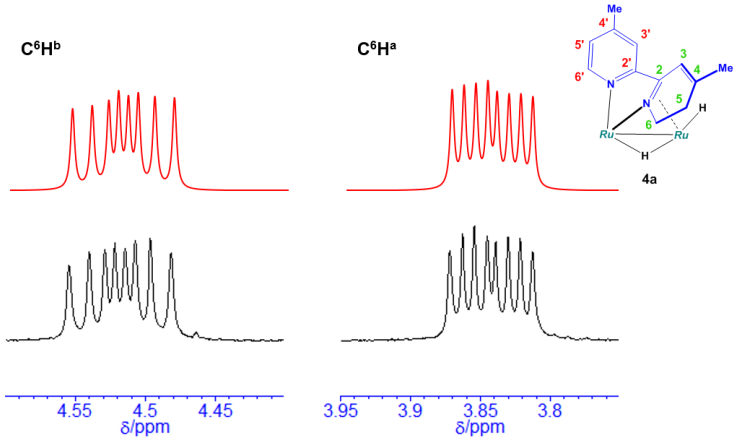

Figure S8. Results of NMR simulations for the methylene protons at the C^6 position of **4a** (red) and observed signals (black) (400 MHz, C_6D_6, 25 °C).

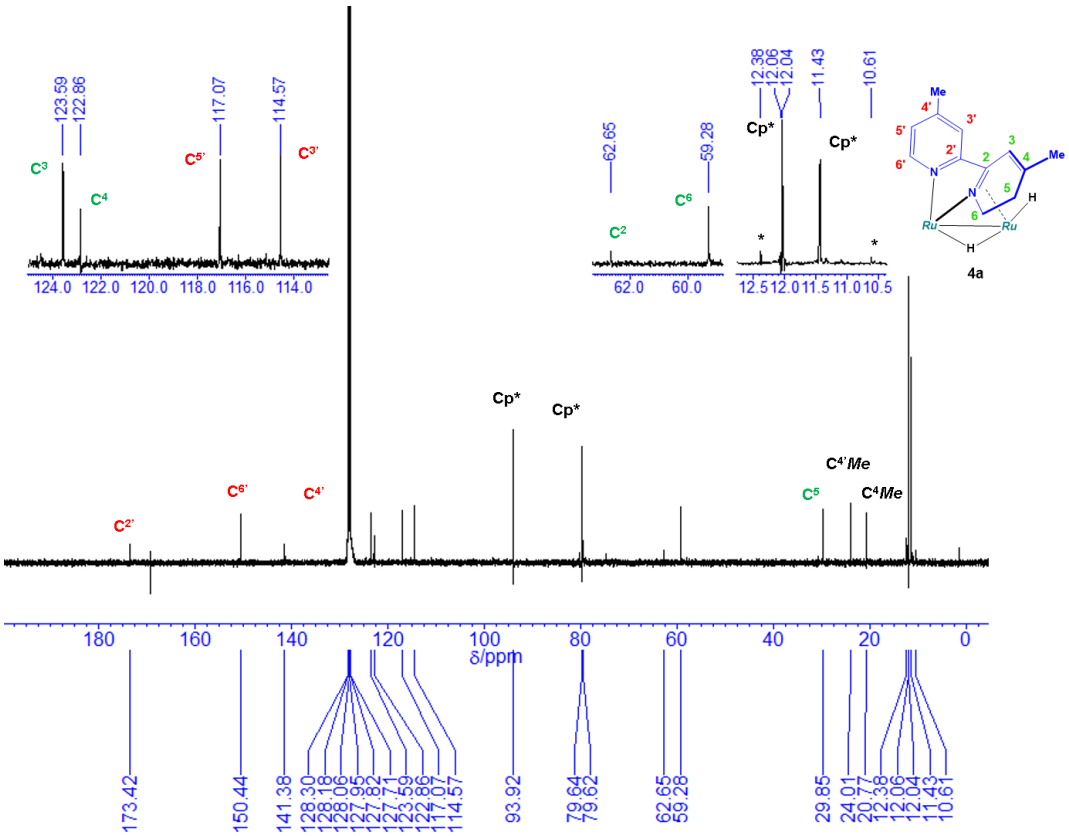

Figure S9. $^{13}C\{^1H\}$ NMR spectrum of **4a** (100 MHz, C_6D_6, 25 °C). The signals with the asterisk were derived from the C_5Me_5 signals of contaminated **5a**.

(c) $(Cp^*Ru)_2\{\mu\text{-}\eta^4\text{-}4,4'\text{-}Me_2dhbpy\}$ (**5a**)

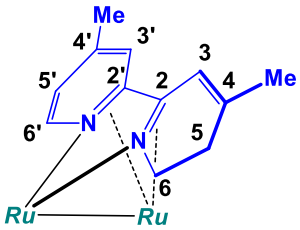

^{1}H NMR (400 MHz, benzene-d_6, 25 ° C): δ 1.5* (m, 1H, C^5H_2), 1.57 (s, 15H, C_5Me_5), 1.73 (s, 3H, C^4Me), 1.9* (m, 1H, C^5H_2), 1.90 (s, 3H, $C^{4'}Me$), 1.98 (s, 15H, C_5Me_5), 3.45 (ddd, J = 13.0, 5.9, 5.8 Hz, 1H, C^6H_2), 3.81 (ddd, J = 13.0, 9.1, 5.1 Hz, 1H, C^6H_2), 5.74 (d, J = 7.2 Hz, 1H, $C^{5'}H$), 6.10 (s, 1H, C^3H), 6.42 (s, 1H, $C^{3'}H$), 7.45 ppm (d, J = 7.2 Hz, 1H, $C^{6'}H$) (* confirmed by H–H COSY). ^{13}C NMR (100 MHz, Benzene-d_6, 25 ° C): δ 10.6 (q, J_{CH} = 127 Hz, C_5Me_5), 12.4 (q, J_{CH} = 125 Hz, C_5Me_5), 20.9 (q, J_{CH} = 128 Hz, $C^{4'}Me$), 23.5 (q, J_{CH} = 132 Hz, C^4Me), 30.7 (dd, J_{CH} = 119, 119 Hz, C^5), 58.1 (dd, J_{CH} = 141, 140 Hz, C^6), 74.7 (s C_5Me_5), 80.2 (s C_5Me_5), 91.5 (s, C^2), 101.3 (s, $C^{2'}$), 111.0 (d, J_{CH} = 168 Hz, $C^{5'}$), 115.2 (d, J_{CH} = 157 Hz, $C^{3'}$), 116.3 (d, J_{CH} = 157 Hz, C^3), 130.7 (s, $C^{4'}$), 131.2 (s, C^4), 151.1 ppm (d, J_{CH} = 177 Hz, $C^{6'}$). IR (KBr, cm^{-1}): 2961, 2910, 1653, 1616, 1507, 1474, 1447, 1376, 1335, 1297, 1025.

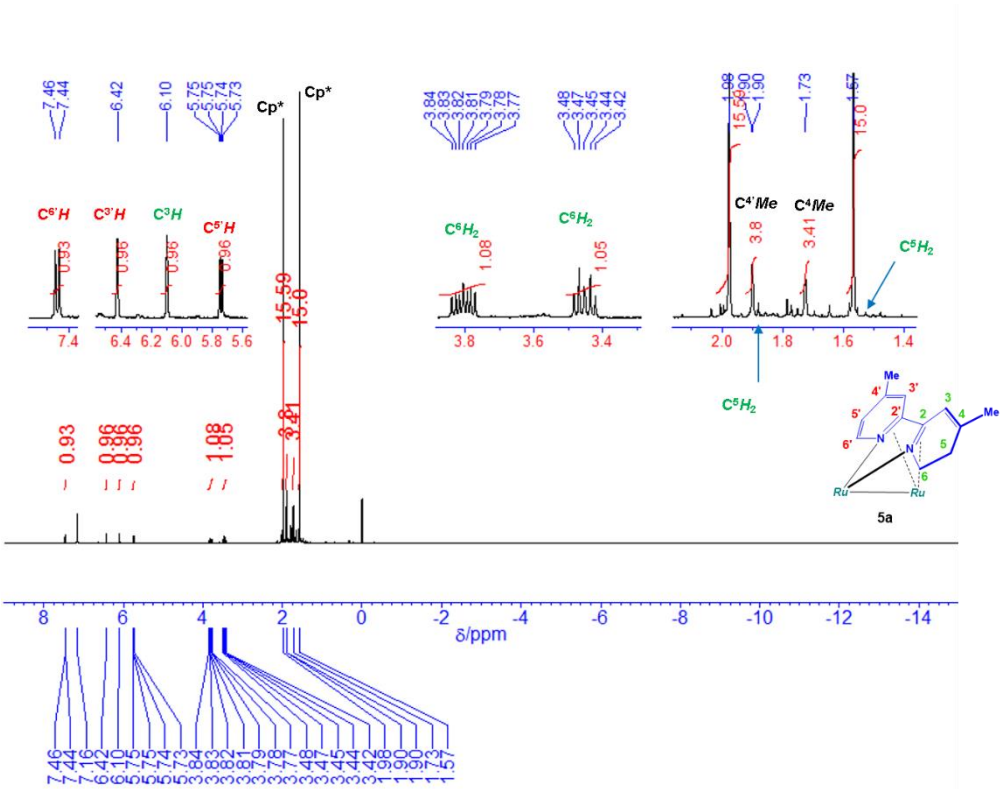

Figure S10. ^{1}H NMR spectrum of **5a** (400 MHz, C_6D_6, 25 °C).

Table S3. Coupling parameters for the methylene protons at the C^6 position of **5a**.

		δ /ppm	W /Hz	*J* [1]	*J* [2]	*J* [3]
1	C^5H^a	(1.500)*	1.40			
2	C^5H^b	(1.900)*	1.40	(16.40)		
3	C^6H^a	3.453	1.40	5.85	5.80	
4	C^6H^b	3.805	1.30	9.05	5.10	13.00

* obscured by the Cp* and Me signals

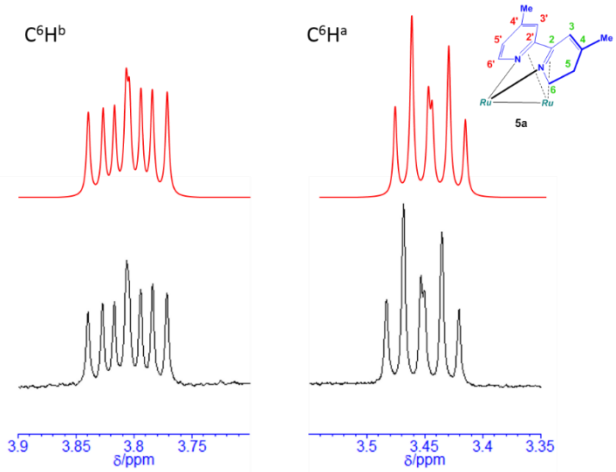

Figure S11. Results of NMR simulations for the methylene protons at the C^6 position of **5a** (red) and observed signals (black) (400 MHz, C_6D_6, 25 °C).

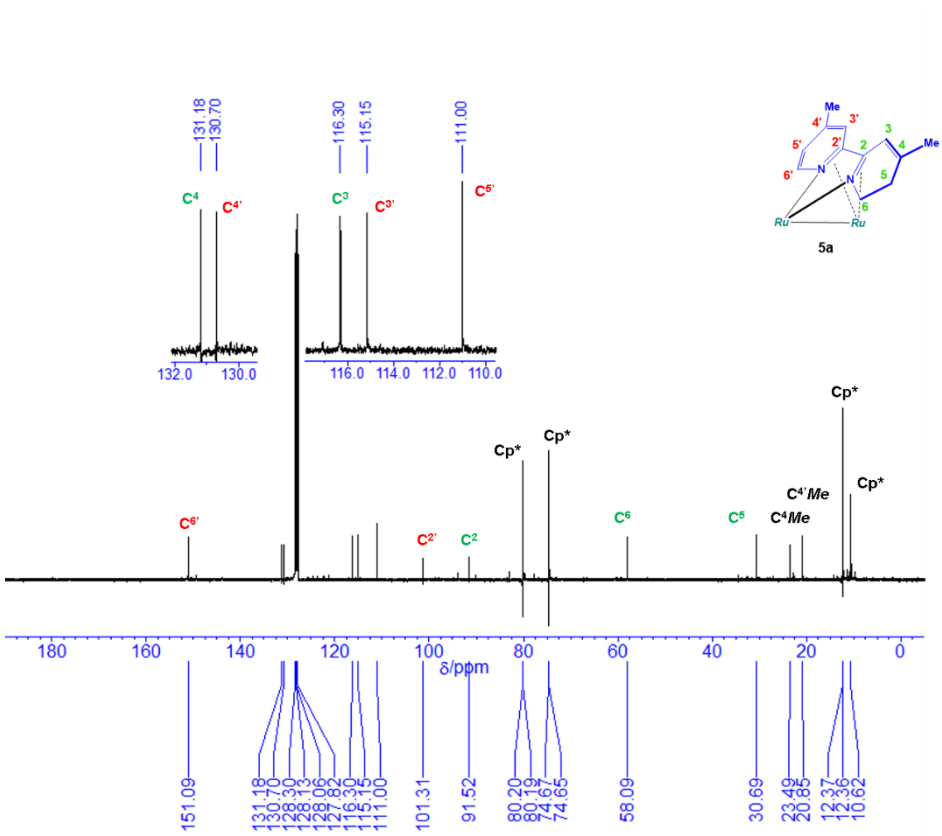

Figure S12. $^{13}C\{^1H\}$ NMR spectrum of **5a** (100 MHz, C_6D_6, 25 °C).

(d) $(Cp^*Ru)_2\{\mu\text{-}\eta^4\text{-}4,4'\text{-}(CF_3)_2dhbpy\}$ (**5b**)

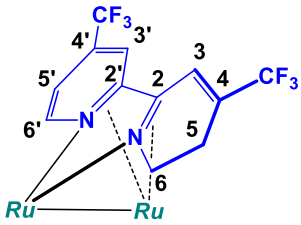

^{1}H NMR (400 MHz, benzene-d_6, 25 ° C): δ 1.37 (s, 15H, C_5Me_5), 1.60 (m, 1H, C^5H_2), 1.80 (s, 15H, C_5Me_5), 2.09 (ddd, J_{HH} = 16.4, 5.3, 4.9 Hz, 1H, C^5H_2), 3.42 (ddd, J_{HH} = 13.5, 5.6, 5.3 Hz, 1H, C^6H_2), 3.64 (ddd, J_{HH} = 13.5, 9.9, 4.9 Hz, 1H, C^6H_2), 5.95 (dd, J_{HH} = 7.1, 2.0 Hz, 1H, $C^{5'}$H), 6.75 (dq, J_{HH} = 2.0 Hz, J_{HF} = 1.8 Hz, 1H, $C^{3'}$H), 6.88 (ddq, J_{HH} = 1.6, 1.1 Hz, J_{HF} = 1.7 Hz, 1H, C^3H), 7.44 ppm (d, J_{HH} = 7.1 Hz, 1H, $C^{6'}$H). ^{13}C NMR (100 MHz, acetone-d_6, 25 ° C): δ 10.4 (q, J_{CH} = 127 Hz, C_5Me_5), 12.0 (q, J_{CH} = 126 Hz, C_5Me_5), 23.3 (t, J_{CH} = 130 Hz, C^5H_2), 57.8 (dd, J_{CH} = 143, 140 Hz, C^6H_2), 76.2 (s C_5Me_5), 81.9 (s, C_5Me_5), 91.3 (s, C^2), 100.9 (s, $C^{2'}$), 103.6 (dq, J_{CH} = 167 Hz, J_{CF} = 3 Hz, $C^{5'}$), 120.0 (dq, J_{CH} = 166 Hz, J_{CF} = 6 Hz, $C^{3'}$), 121.2 (q, J_{CF} = 32 Hz, $C^{4'}$), 123.3 (q, J_{CF} = 33 Hz, C^4), 124.9 (q, J_{CF} = 270 Hz, CF_3), 125.4 (dq, J_{CH} = 164 Hz, J_{CF} = 6 Hz, C^3), 125.7 (q, J_{CF} = 269 Hz, CF_3), 153.1 ppm (d, J_{CH} = 182 Hz, $C^{6'}$). ^{19}F{^{1}H} NMR (377 MHz, benzene-d_6, 25 ° C): δ –65.9 (s, CF_3), –63.9 ppm (s, CF_3).

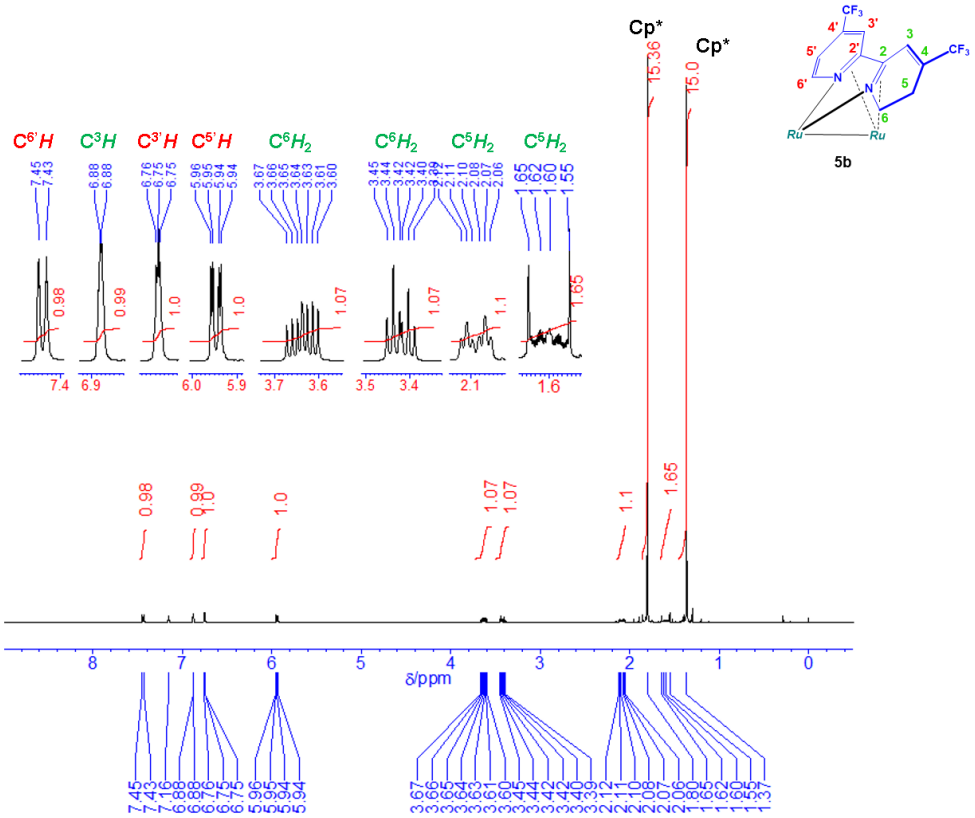

Figure S13. ^{1}H NMR spectrum of **5b** (400 MHz, C_6D_6, 25 °C).

Table S4. Coupling parameters for the methylene protons at the C^5 and C^6 positions of **5b**.

		δ /ppm	W /Hz	*J* [1]	*J* [2]	*J* [3]	*J* [4]
1	C^5H^a	1.601	1.40				
2	C^5H^b	2.089	1.40	16.40			
3	C^6H^a	3.422	1.40	5.60	5.30		
4	C^6H^b	3.636	1.30	9.90	4.90	13.50	
5	^{19}F	(–63.9)		1.85	0.90	0.00	0.00

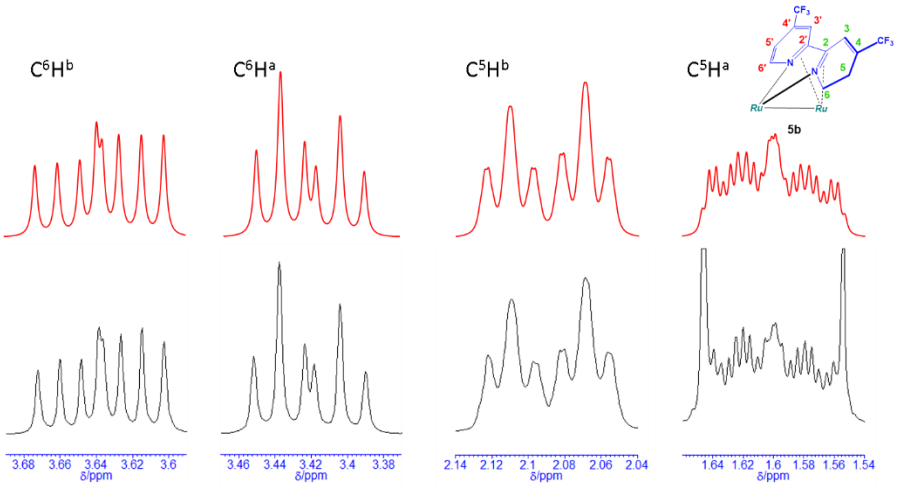

Figure S14. Results of NMR simulations for the methylene protons at the C^5 and C^6 positions of **5b** (red) and observed signals (black) (400 MHz, C_6D_6, 25 °C).

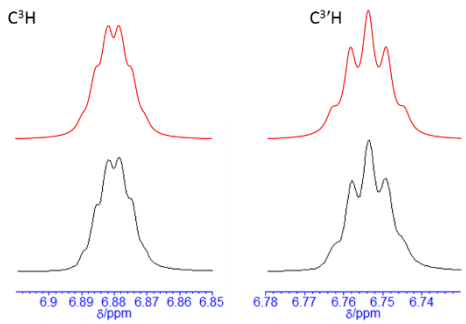

Figure S15. Results of NMR simulations for the methylene protons at the C^3 and $C^{3'}$ positions of **5b** (red) and observed signals (black): C^3H: J_{HH} = 1.60, 1.10 Hz; J_{HF} = 1.65 Hz, $C^{3'}H$: J_{HH} = 2.0 Hz; J_{HF} = 1.80 Hz. (400 MHz, C_6D_6, 25 °C).

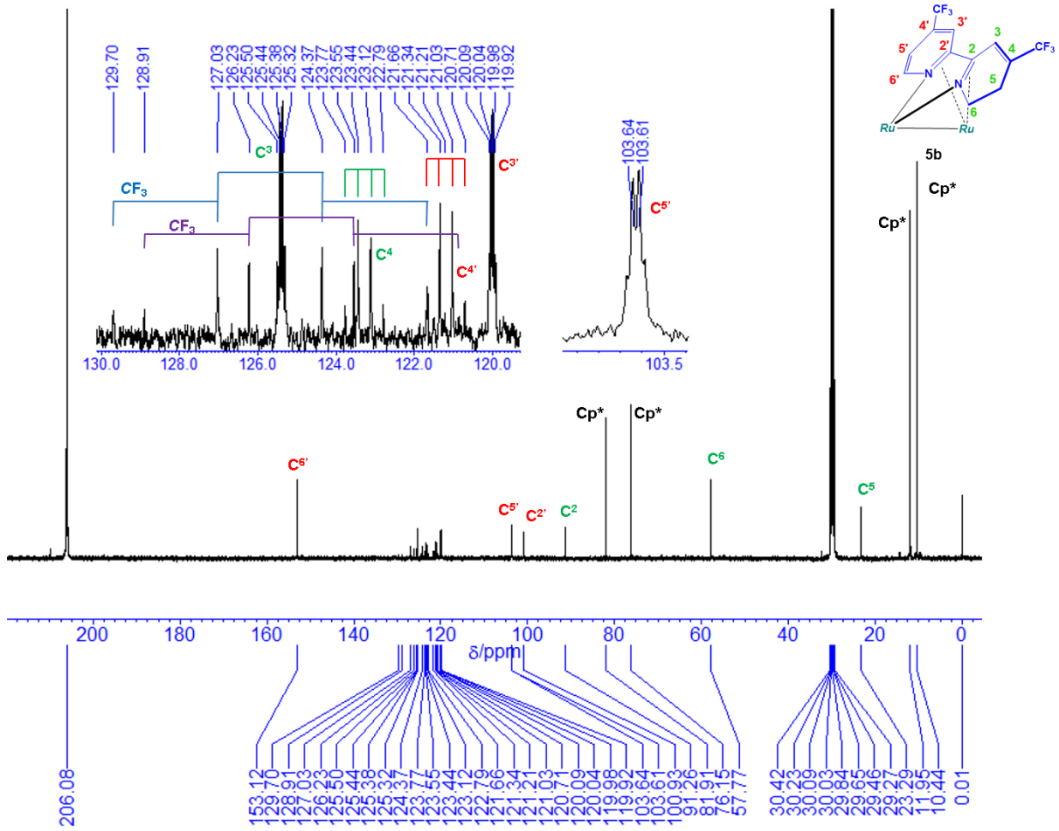

Figure S16. $^{13}C\{^{1}H\}$ NMR spectrum of **5b** (100 MHz, acetone-d_6, 25 °C).

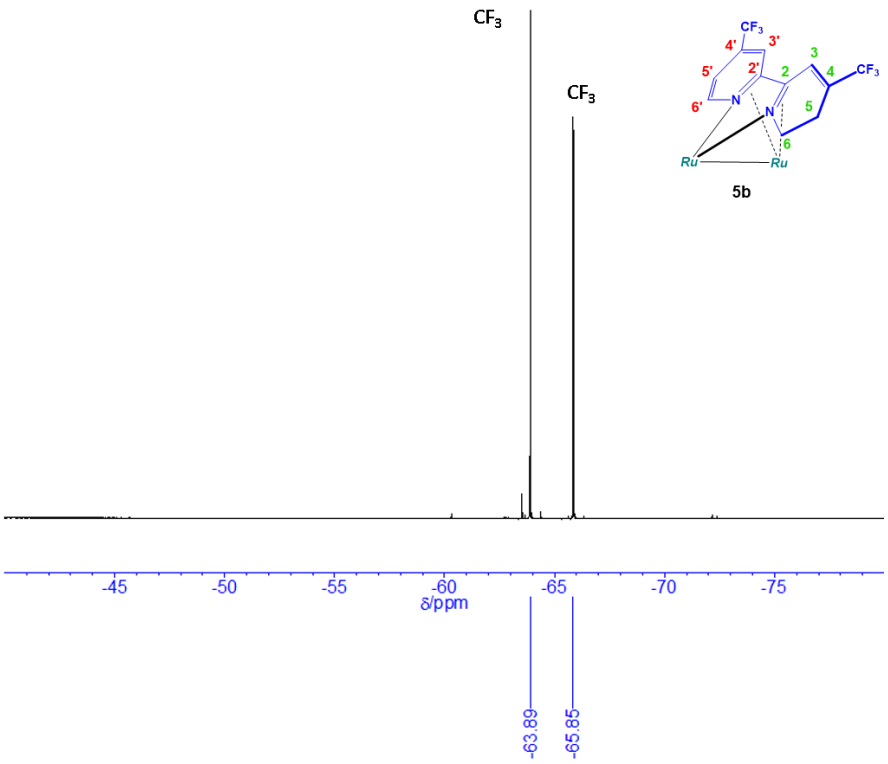

Figure S17. $^{19}F\{^{1}H\}$ NMR spectrum of **5b** (377 MHz, C_6D_6, 25 °C).

(e) $(Cp^*Ru)_2\{\mu\text{-}\eta^4\text{-}4,4'\text{-}(COOEt)_2dhbpy\}$ (**5c**)

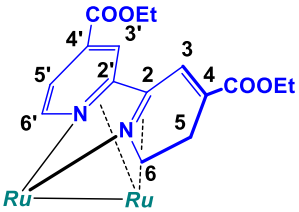

^{1}H NMR (400 MHz, benzene-d_6, 25 ° C): δ 0.98 (t, J = 7.2 Hz, 3H, CH_2CH_3), 1.04 (t, J = 7.2 Hz, 3H, CH_2CH_3), 1.41 (s, 15H, C_5Me_5), 1.83 (s, 15H, C_5Me_5), 1.88* (m, 1H, C^5H_2), 2.68 (ddd, J = 15.6, 5.4, 4.9 Hz, 1H, C^5H_2), 3.62 (ddd, J = 13.4, 5.4, 5.0 Hz,1H, C^6H_2), 3.72 (ddd, J = 13.4, 10.5, 4.9 Hz, 1H, C^6H_2), 4.03–4.20 (m, 4H, CH_2CH_3), 6.78 (d, J = 7.2 Hz, 1H, $C^{5'}H$), 7.57 (d, J = 7.2 Hz, 1H, $C^{6'}H$), 7.83 (s, 1H, C^3H), 7.92 ppm (s, 1H, $C^{3'}H$) (* confirmed by H–H COSY). ^{13}C NMR (100 MHz, benzene-d_6, 25 ° C): δ 10.3 (q, J_{CH} = 126 Hz, C_5Me_5), 12.0 (q, J_{CH} = 126 Hz, C_5Me_5), 14.4 (q, J_{CH} = 132 Hz, CH_2CH_3), 14.5 (q, J_{CH} = 126 Hz, CH_2CH_3), 24.9 (dd, J_{CH} = 131, 126 Hz, C^5), 58.1 (dd, J_{CH} = 139, 139 Hz, C^6), 60.2 (t, J_{CH} = 143 Hz, CH_2CH_3), 60.6 (t, J_{CH} = 145 Hz, CH_2CH_3), 76.0 (s C_5Me_5), 81.2 (s, C_5Me_5), 92.7 (s, C^2), 102.7 (s, $C^{2'}$), 107.3 (d, J_{CH} = 169 Hz, $C^{5'}$), 122.2 (s, C^4), 123.2 (s, $C^{4'}$), 126.2 (d, J_{CH} = 166 Hz, $C^{3'}$), 131.3 (d, J_{CH} = 162 Hz, C^3), 150.9 (d, J_{CH} = 181 Hz, $C^{6'}$), 165.1 (s, COOEt), 166.7 ppm (s, COOEt).

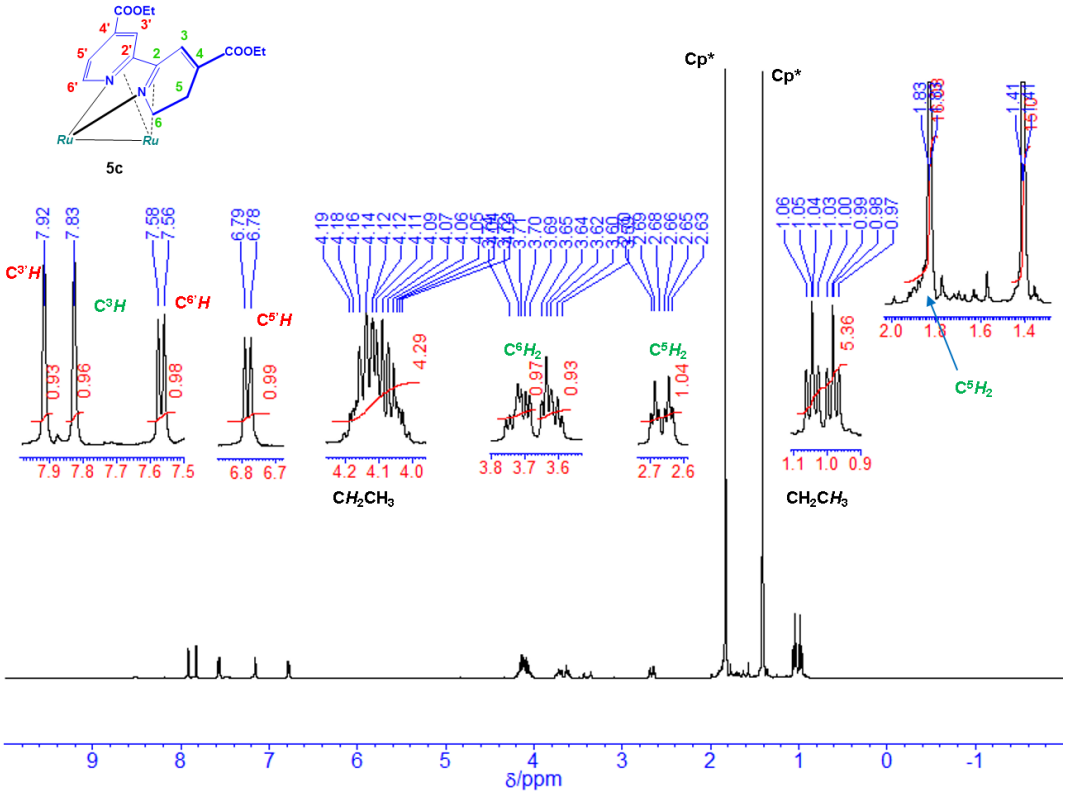

Figure S18. ^{1}H NMR spectrum of **5c** (400 MHz, C_6D_6, 25 °C).

Table S5. Coupling parameters for the methylene protons at the C^5 and C^6 positions of **5c**.

		δ /ppm	W /Hz	*J* [1]	*J* [2]	*J* [3]
1	C^5H^a	(1.874)*	1.40			
2	C^5H^b	2.675	1.40	15.6		
3	C^6H^a	3.622	1.30	5.00	5.40	
4	C^6H^b	3.717	1.30	10.50	4.90	13.40

* obscured by the Cp* signal

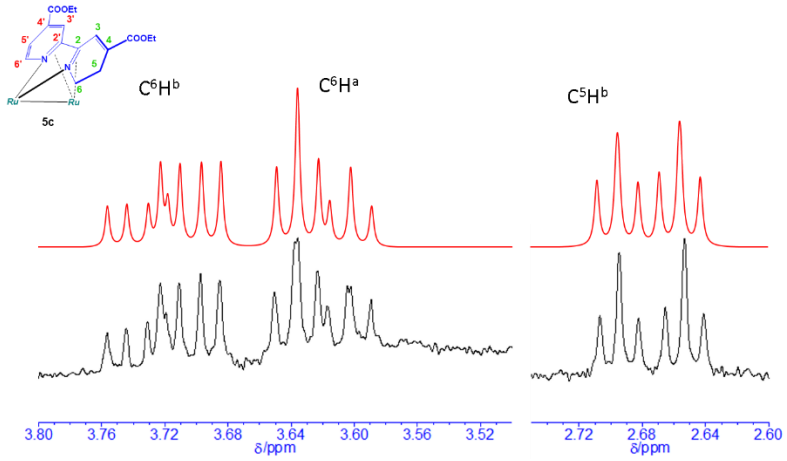

Figure S19. Results of NMR simulations for the methylene protons at the C^5 and C^6 positions of **5c** (red) and observed signals (black) (400 MHz, C_6D_6, 25 °C).

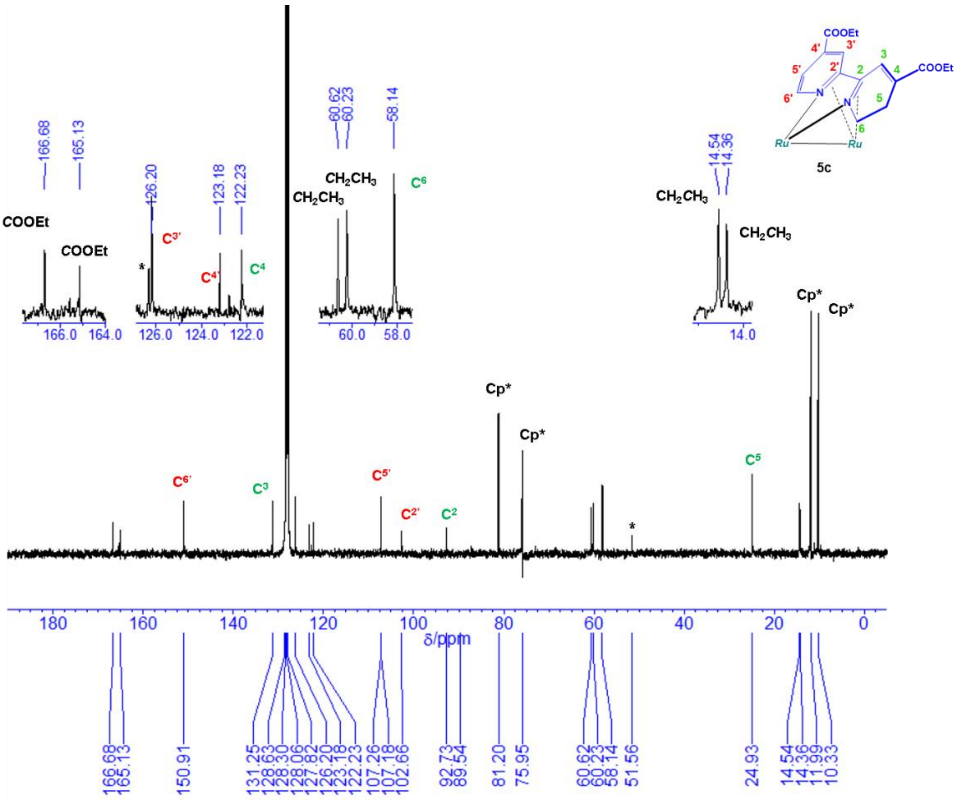

Figure S20. $^{13}C\{^1H\}$ NMR spectrum of **5c** (100 MHz, C_6D_6, 25 °C).

(f) $(Cp^*Ru)_2\{\mu\text{-}\eta^2\text{-}4,4'\text{-}(CF_3)_2dhbpy\}(\mu\text{-}H)(H)$ (**4b**)

^{1}H NMR (400 MHz, benzene-d_6, 25 °C): δ –14.89 (d, J = 5.1 Hz, 1H, RuH), –11.26 (d, J = 5.1 Hz, 1H, RuH), 1.58 (s, 15H, C_5Me_5), 1.72 (s, 15H, C_5Me_5), 4.15 (m, 1H, C^6H_2), 6.85 (s, 1H, C^3H or $C^{3'}H$), 7.07 (s, 1H, C^3H or $C^{3'}H$), 7.83 ppm (d, J = 6.0 Hz, $C^{6'}H$). Other methylene signals derived from C^5H_2 and C^6H_2 could not be detected owing to the obstruction by the signals derived from **5b**.

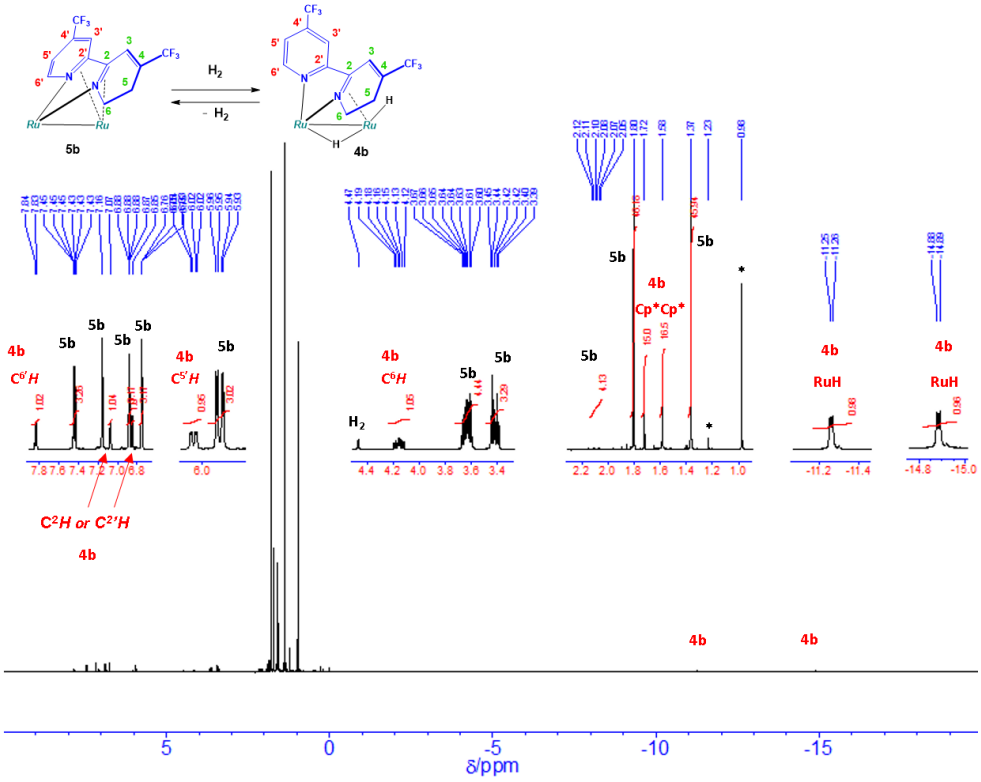

Figure S21. ^{1}H NMR spectrum of the mixture obtained by the reaction of **5b** with 1 atm of H_2 at 40 °C; recorded after 24 h (400 MHz, C_6D_6, 25 °C). Signals with an asterisk were derived from 2,2′,4,4′-tetramethylpentane used for an internal standard.

(g) $(Cp^*Ru)_2\{\mu\text{-}\eta^2\text{-}4,4'\text{-}(COOEt)_2dhbpy\}(\mu\text{-}H)(H)$ (**4c**)

^{1}H NMR (400 MHz, benzene-d_6, 25 °C): δ –14.79 (d, J = 4.5 Hz, 1H, RuH), –11.16 (d, J = 4.5 Hz, 1H, RuH), 0.88 (t, J = 7.1 Hz, 3H, CH_2CH_3), 1.11 (t, J = 7.1 Hz, 3H, CH_2CH_3), 1.62 (s, 15H, C_5Me_5), 1.73 (s, 15H, C_5Me_5), 2.78 (dd, J = 16.7, 5.4 Hz, 1H, C^5H_2), 3.2–3.4 (m, 1H, C^6H_2), 3.93 (q, J = 7.1 Hz, 2H, CH_2CH_3), 6.93 (d, J = 5.9 Hz, 1H, $C^{5'}H$), 7.75 (s, C^3H), 8.02 (d, J = 5.9 Hz, 1H, $C^{6'}H$), 8.10 ppm (s, 1H, $C^{3'}H$). Other methylene signals derived from C^5H_2, C^6H_2, and $COOCH_2CH_3$ could not be detected owing to the obstruction by the signals derived from **5c**.

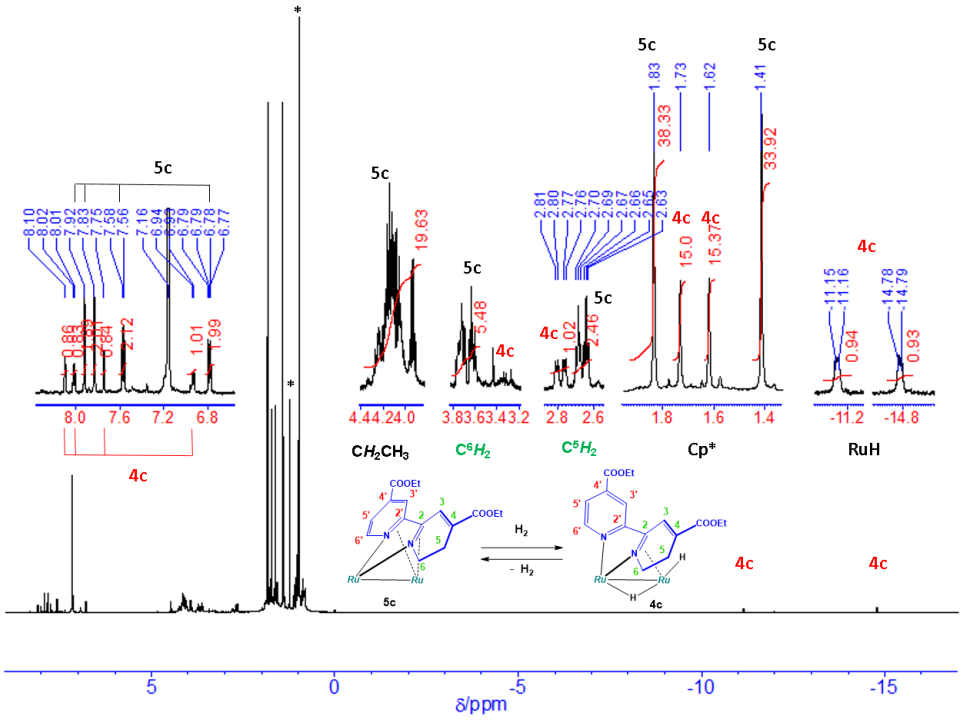

Figure S22. ^{1}H NMR spectrum of the mixture obtained by the reaction of **5c** with 1 atm of H_2 at 40 °C; recorded after 24 h (400 MHz, C_6D_6, 25 °C). Signals with an asterisk were derived from 2,2′,4,4′-tetra-methylpentane used for an internal standard.

(h) $(Cp^*Ru)_2(\mu\text{-}\eta^4\text{-}4,4'\text{-}Me_2dhbpy)(^tBuNC)$ **(6a)**

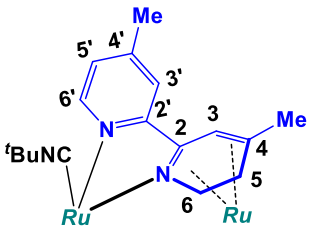

^{1}H NMR (400 MHz, benzene-d_6, 25 ° C): δ 1.04 (s, 9H, ^{t}*Bu*NC), 1.6* (C^5H_2), 1.69 (s, 15H, C_5Me_5), 1.73 (s, 15H, C_5Me5), 1.93 (s, 6H, *Me*), 2.2* (C^5H_2), 2.48 (ddd, J = 11.5, 7.9, 6.2 Hz, 1H, C^6H_2), 2.81 (ddd, J = 11.5, 8.6, 3.1 Hz, 1H, C^6H_2), 4.47 (s, 1H, C^3H), 6.10 (dd, J = 5.9, 1.7 Hz, 1H, $C^{5'}H$), 6.62 (m, 1H, $C^{3'}H$), 7.83 ppm (d, J = 5.8 Hz, 1H, $C^{6'}H$).

^{13}C NMR (100 MHz, benzene-d_6, 25 ° C): δ 10.7 (q, J_{CH} = 126 Hz, C_5Me_5), 11.7 (q, J_{CH} = 125 Hz, C_5Me_5), 20.9 (q, J_{CH} = 127 Hz, C^4Me or C4′Me), 27.3 (q, J_{CH} = 123 Hz, C4*Me* or C4′*Me*), 31.7 (q, J_{CH} = 128 Hz, Me_3CNC), 44.4 (t, J_{CH} = 124 Hz, C^5), 55.6 (s, Me_3*C*NC), 59.2 (t, J_{CH} = 135 Hz, C^6), 59.7 (s, C^4), 71.5 (d, J_{CH} = 163 Hz, C^3), 82.5 (s, C_5Me_5), 87.3 (s, C_5Me_5), 94.5 (s, C^2), 114.0 (d, J_{CH} = 160 Hz, $C^{3'}$), 115.9 (d, J_{CH} = 162 Hz, $C^{5'}$), 143.7 (t, J_{CH} = 6 Hz, $C^{4'}$), 150.8 (dd, J_{CH} = 176, 4 Hz, $C^{6'}$), 168.9 (d, J_{CH} = 8 Hz, $C^{2'}$), 176.2 ppm (s, ^{t}BuN*C*).

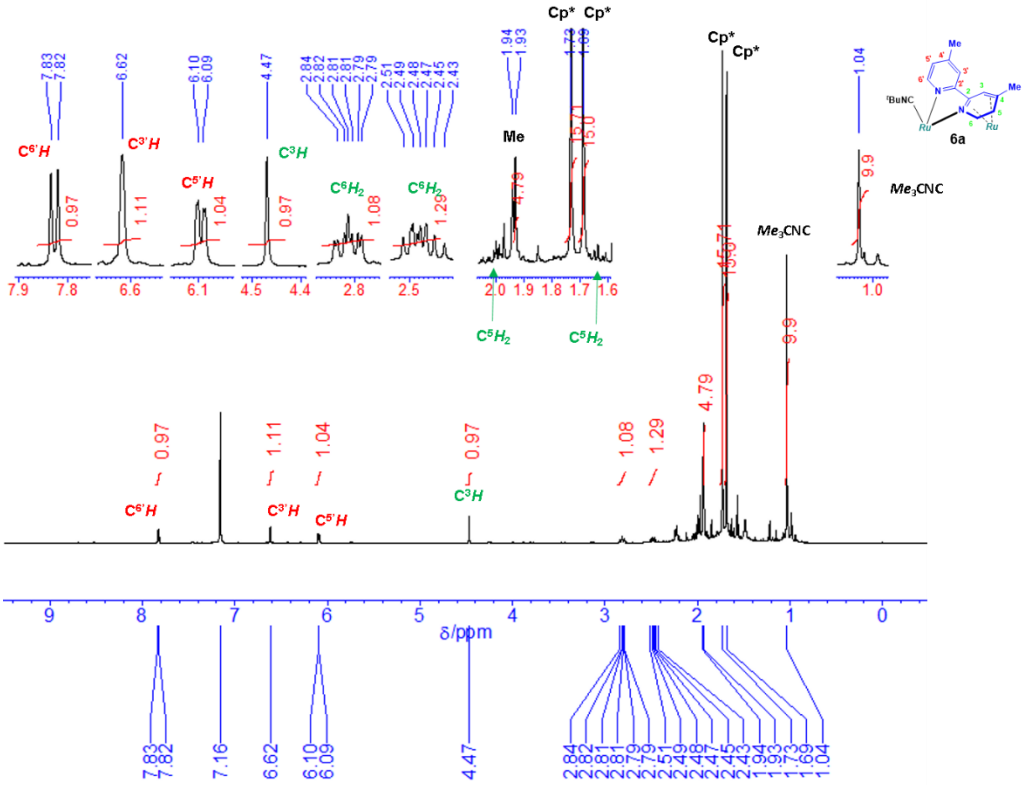

Figure S23. ^{1}H NMR spectrum of **6a** (400 MHz, C_6D_6, 25 °C).

Table S6. Coupling parameters for the methylene protons at the C^6 position of **6a**.

		δ /ppm	W /Hz	*J* [1]	*J* [2]	*J* [3]
1	C^5H^a	(2.040)*	1.40			
2	C^5H^b	(2.200)	1.40	(11.00)		
3	C^6H^a	2.481	2.10	6.20	7.90	
4	C^6H^b	2.813	2.00	3.10	8.60	11.50

obscured by the Cp and methyl signals.

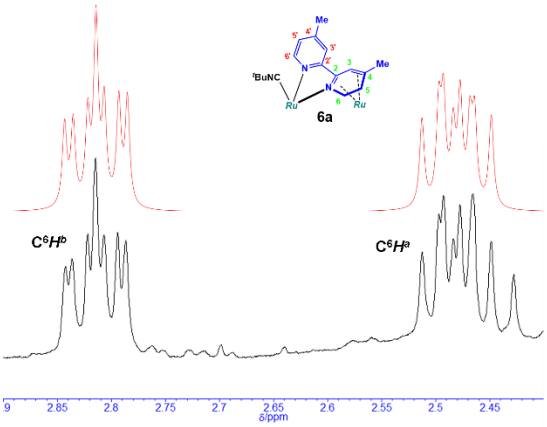

Figure S24. Results of NMR simulations for the methylene protons at the C^6 position of **6a** (red) and observed signals (black) (400 MHz, C_6D_6, 25 °C).

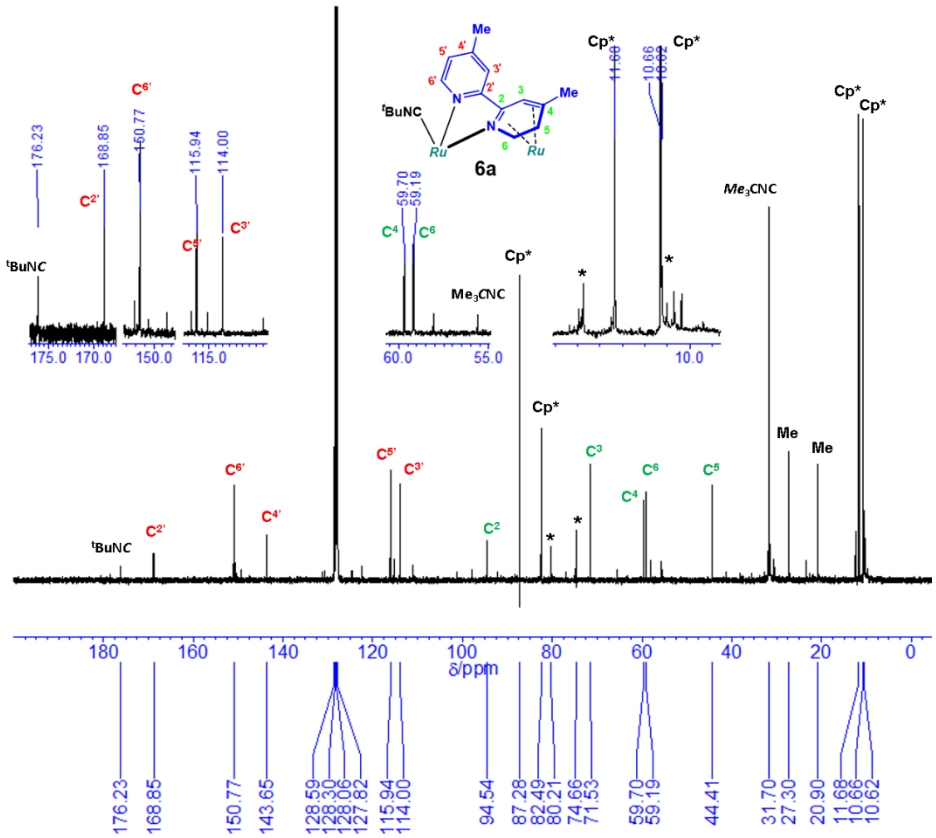

Figure S25. $^{13}C\{^1H\}$ NMR spectrum of **6a** (100 MHz, C_6D_6, 25 °C). Asterisked signals were derived from **5a**. The signals with an asterisk were derived from the Cp* groups of contaminated **5a**.

(i) $(Cp^*Ru)_2\{\mu\text{-}\eta^4\text{-}4,4'\text{-}(CF_3)_2dhbpy\}(^tBuNC)$ (**6b**)

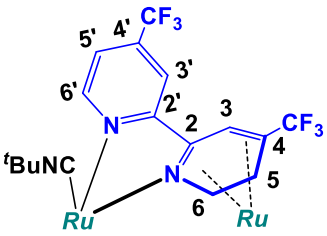

^{1}H NMR (400 MHz, benzene-d_6, 25 ° C): δ 0.91 (s, 9H, ^{t}*Bu*NC), 1.55 (s, 15H, C_5*Me*$_5$), 1.64 (s, 15H, C_5*Me*$_5$), 2.19 (ddd, J = 11.6, 10.5, 7.2 Hz, 1H, C^5H_2), 2.31 (ddd, J = 11.2, 7.2, 6.4 Hz, 1H, C^6H_2), 2.39 (ddd, J = 11.6, 6.4, 1.5 Hz, 1H, C^5H_2), 2.76 (ddd, J = 11.2, 10.5, 1.5 Hz, 1H, C^6H_2), 5.12 (s, C^3H), 6.25 (dd, J = 6.1, 2.0 Hz, 1H, $C^{5'}H$), 7.02 (m, $C^{3'}H$), 7.84 ppm (d, J = 6.1 Hz, 1H, $C^{6'}H$). $^{13}C\{^1H\}$ NMR (100 MHz, acetone-d_6, 25 ° C): δ 10.7 (C_5*Me*$_5$), 11.3 (C_5*Me*$_5$), 31.7 (^{t}BuNC), 35.0 (q, J_{CF} = 2 Hz, C^3), 54.5 (q, J_{CF} = 31 Hz, C^4), 57.0 (Me_3*C*NC), 59.1 (*C*^{6}), 68.8 (q, J_{CF} = 5 Hz, *C*^{5}), 85.0 (*C*$_5$Me$_5$), 87.7 (*C*$_5$Me$_5$), 95.7 (*C*^{2}), 111.0 (q, J_{CF} = 4 Hz, $C^{3'}$or $C^{5'}$), 111.2 (q, J_{CF} = 4 Hz, $C^{3'}$or $C^{5'}$), 124.6 (q, J_{CF} = 272 Hz, *C*F$_3$), 135.0 (q, J_{CF} = 274 Hz, *C*F$_3$), 136.2 (q, J_{CF} = 33 Hz, *C*$^{4'}$), 153.4 (*C*$^{6'}$), 169.0 (*C*$^{2'}$), 210.0 ppm (^{t}BuN*C*). $^{19}F\{^1H\}$ NMR (377 MHz, benzene-d_6, 25 ° C): δ –64.0 (s, C*F*$_3$), –60.2 ppm (s, C*F*$_3$).

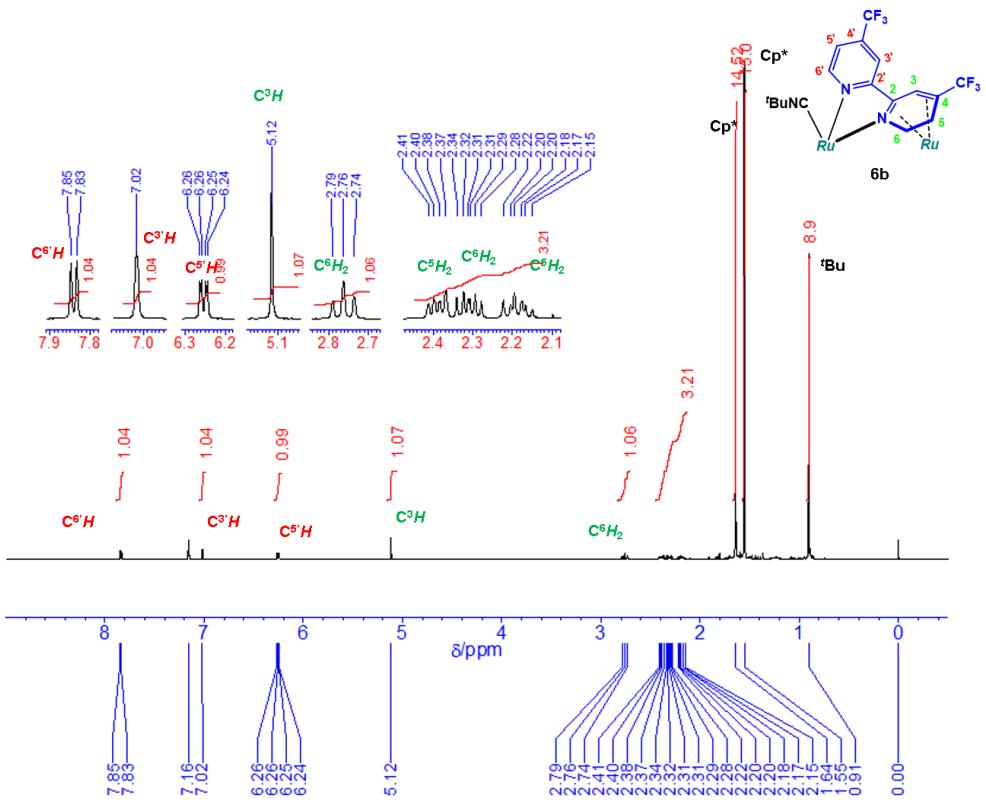

Figure S26. ^{1}H NMR spectrum of **6b** (400 MHz, C_6D_6, 25 °C).

Table S7. Coupling parameters for the methylene protons at the C^5 and C^6 positions of **6b**.

		δ /ppm	W /Hz	*J* [1]	*J* [2]	*J* [3]	*J* [4]
1	C^5H^a	2.189	1.50				
2	C^6H^a	2.310	1.50	7.20			
3	C^5H^b	2.390	1.50	–11.60	6.40		
4	C^6H^b	2.761	1.50	10.50	–11.20	1.50	
5	^{19}F	----	----	0.50	0.00	0.50	0.00

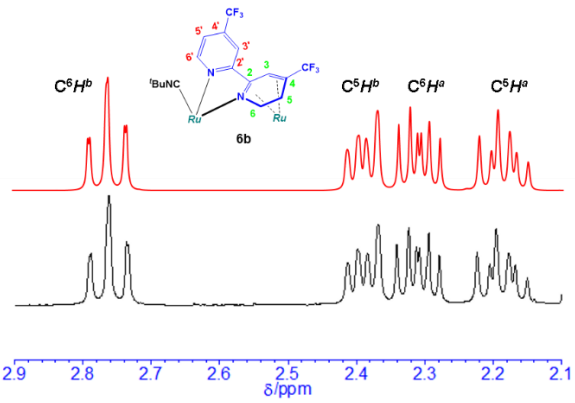

Figure S27. Results of NMR simulations for the methylene protons at the C^5 and C^6 positions of **6b** (red) and observed signals (black) (400 MHz, C_6D_6, 25 °C).

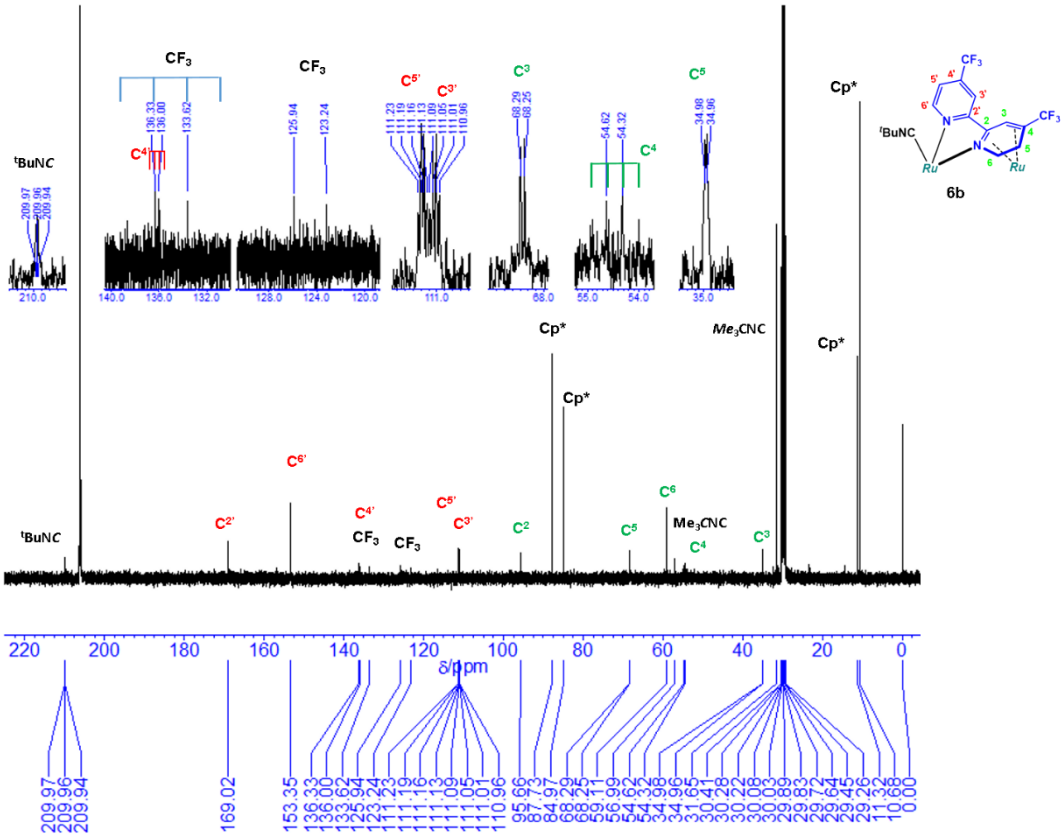

Figure S28. $^{13}C\{^1H\}$ NMR spectrum of **6b** (100 MHz, acetone-d_6, 25 °C).

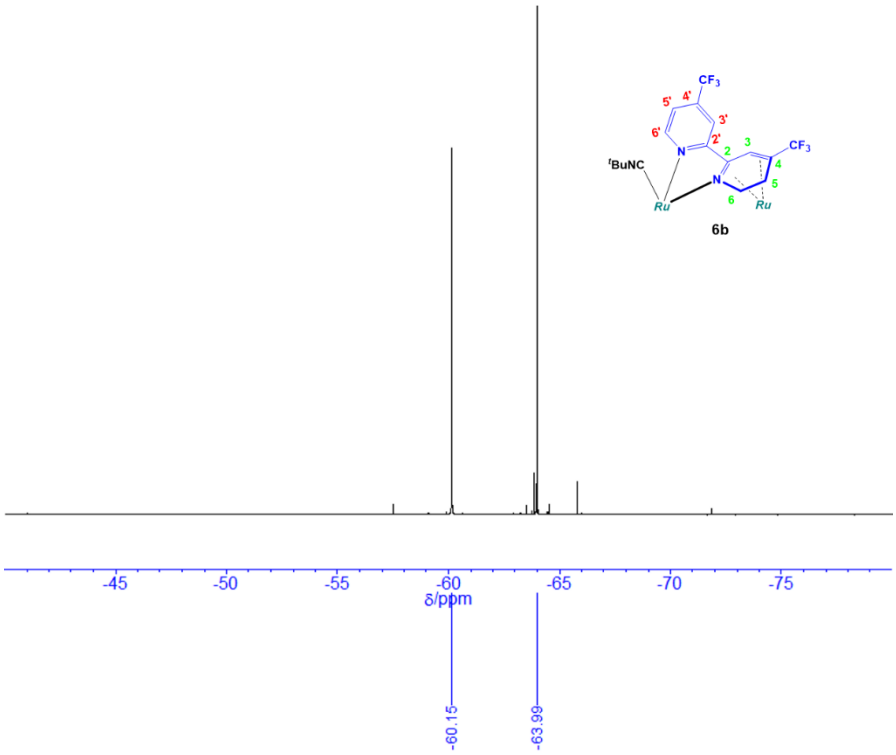

Figure S29. $^{19}F\{^{1}H\}$ NMR spectrum of **6b** (377 MHz, C_6D_6, 25 °C).

(j) $(Cp^*Ru)_2(\mu\text{-}\eta^4\text{-}4,4'\text{-}Me_2bpy)$ (**7a**)

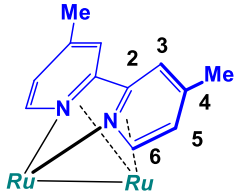

^{1}H NMR (400 MHz, benzene-d_6, 25 °C): δ 1.48 (s, 15H, C_5Me_5), 1.96 (d, J = 1.1 Hz, 6H, C^4Me), 1.98 (s, 15H, C_5Me_5), 5.73 (dd, J = 6.9, 1.8 Hz C^5H), 6.63 (m, 2H, C^3H), 7.62 ppm (d, J = 6.9 Hz, 2H, C^6H). ^{13}C NMR (100 MHz, benzene-d_6, 25 °C): δ 10.1 (q, J_{CH} = 125 Hz, C_5Me_5), 12.2 (q, J_{CH} = 124 Hz, C_5Me_5), 21.0 (q, J_{CH} = 125 Hz, C^4Me), 74.9 (s C_5Me_5), 79.2 (s, C_5Me_5), 96.7 (s, C^2), 111.1 (d, J_{CH} = 159 Hz, C^5), 115.5 (d, J_{CH} = 158 Hz, C^3), 129.7 (s, C^4), 150.8 ppm (d, J_{CH} = 176 Hz, C^6). IR (KBr, cm^{-1}): 2959, 2910, 1654, 1616, 1474, 1448, 1377, 1027, 824.

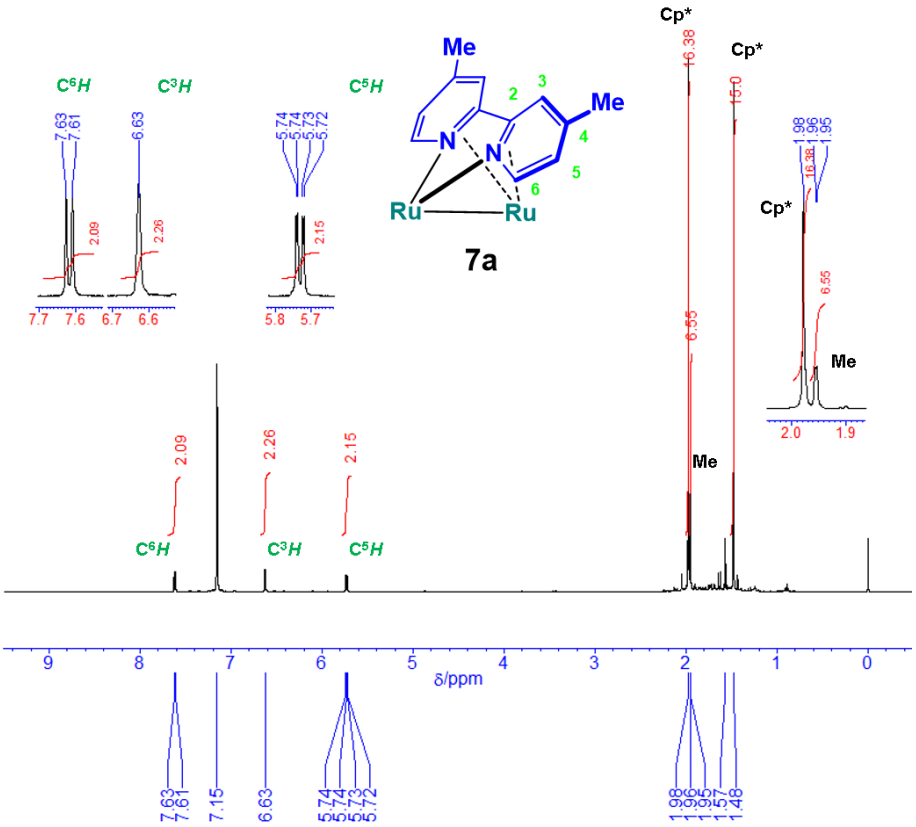

Figure S30. ^{1}H NMR spectrum of **7a** (400 MHz, C_6D_6, 25 °C).

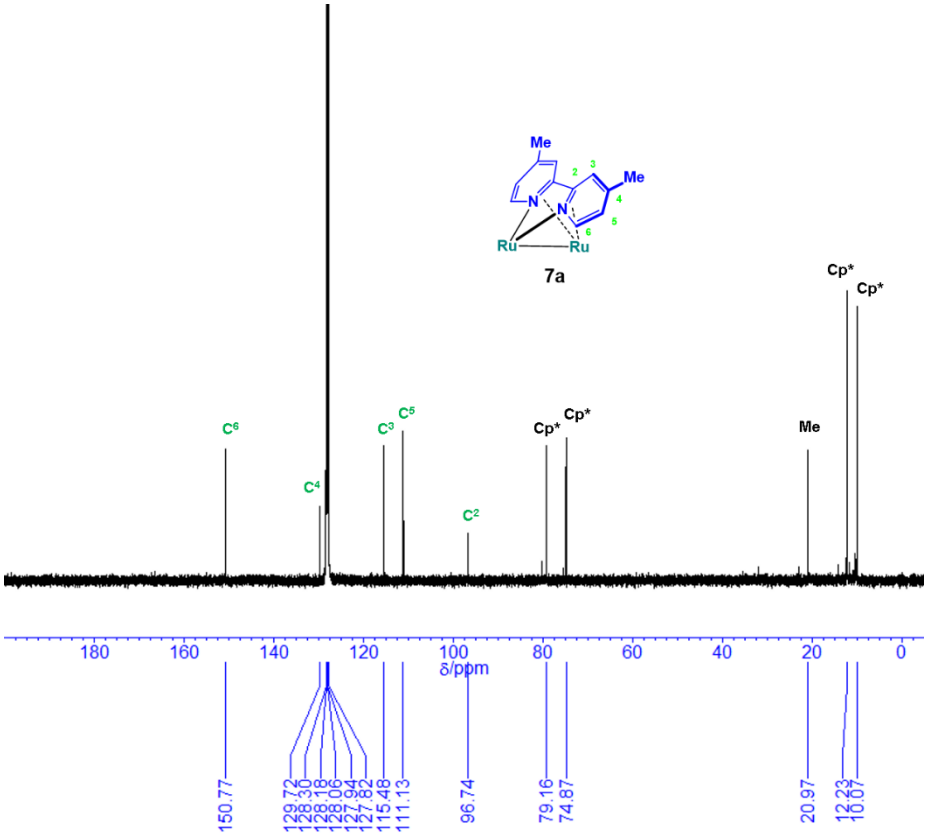

Figure S31. $^{13}C\{^{1}H\}$ NMR spectrum of **7a** (100 MHz, C_6D_6, 25 °C).

(k) $(Cp^*Ru)_2\{\mu\text{-}\eta^4\text{-}4,4'\text{-}(CF_3)_2bpy)\}$ (**7b**)

^{1}H NMR (400 MHz, benzene-d_6, 25 °C): δ 1.30 (s, 15H, C_5Me_5), 1.81 (d, J = 1.1 Hz, 6H, C^4Me), 1.98 (s, 15H, C_5Me_5), 5.94 (dd, J = 7.1, 2.0 Hz C^5H), 7.10 (m, 2H, C^3H), 7.60 ppm (d, J = 7.1 Hz, 2H, C^6H).

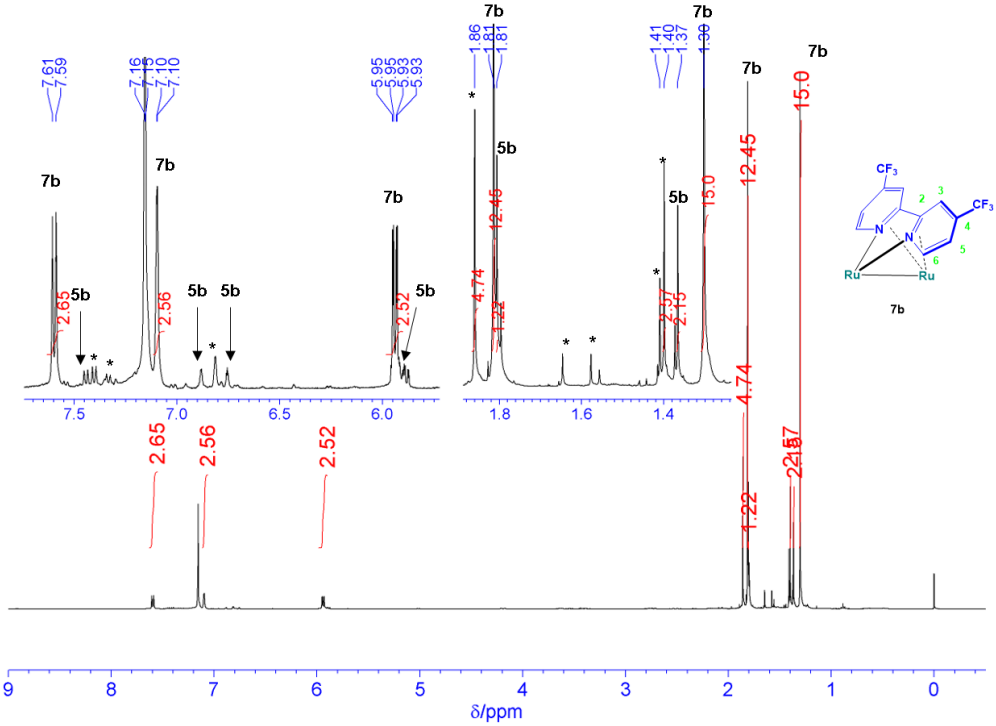

Figure S32. ^{1}H NMR spectrum of the mixture obtained by the thermolysis of **5b** at 140 °C under reduced pressure; recorded after 6 days (400 MHz, C_6D_6, 25 °C). The signals with an asterisk were derived from unidentified products.

(l) $(Cp^*Ru)_2(\mu\text{-}\eta^2\text{-phen})(\mu\text{-H})(H)$ (**8**)

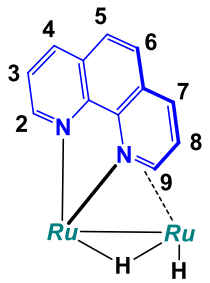

^{1}H NMR (400 MHz, THF-d_8, –25 ° C): δ–13.52 (d, J = 2.0 Hz, 1H, RuH), –13.39 (dd, J = 2.5, 2.0 Hz, 1H, RuH), 1.16 (s, 15H, C_5Me_5), 1.67 (s, 15H, C_5Me_5), 4.35 (dd, J = 3.8, 2.5, 1H, C^9H), 6.84 (d, J = 8.9 Hz, 1H, C^7H), 6.87 (dd, J = 8.9, 3.8 Hz, 1H, C^8H), 7.13 (d, J = 8.2 Hz, 1H, C^5H or C^6H), 7.15 (dd, J = 8.0, 4.9 Hz, 1H, C^3H), 7.37 (d, J = 8.2 Hz, 1H, C^5H or C^6H), 7.84 (d, J = 8.0 Hz, 1H, C^4H), 9.11 ppm (d, J = 4.9 Hz, 1H, C^2H). ^{13}C NMR (100 MHz, THF-d_8, 25 ° C): δ 10.8 (q, J_{CH} = 126 Hz, C_5Me_5), 11.0 (q, J_{CH} = 126 Hz, C_5Me_5), 63.3 (d, J_{CH} = 181 Hz, C^9), 82.1 (s, C_5Me_5), 93.0 (s, C_5Me_5), 114.1 (d, J_{CH} = 161 Hz), 118.7 (d, J_{CH} = 161 Hz), 121.1 (s,), 121.2 (d, J_{CH} = 163 Hz), 126.8 (d, J_{CH} = 157 Hz), 128.2 (d, J_{CH} = 163 Hz), 130.7 (s), 139.9 (d, J_{CH} = 159 Hz), 144.1 (s), 149.3 (d, J_{CH} = 149 Hz), 150.9 ppm (s). Signals derived from the phenanthroline moiety could not be assigned except for the C^9 signal that was π-bonded to the Ru centre.

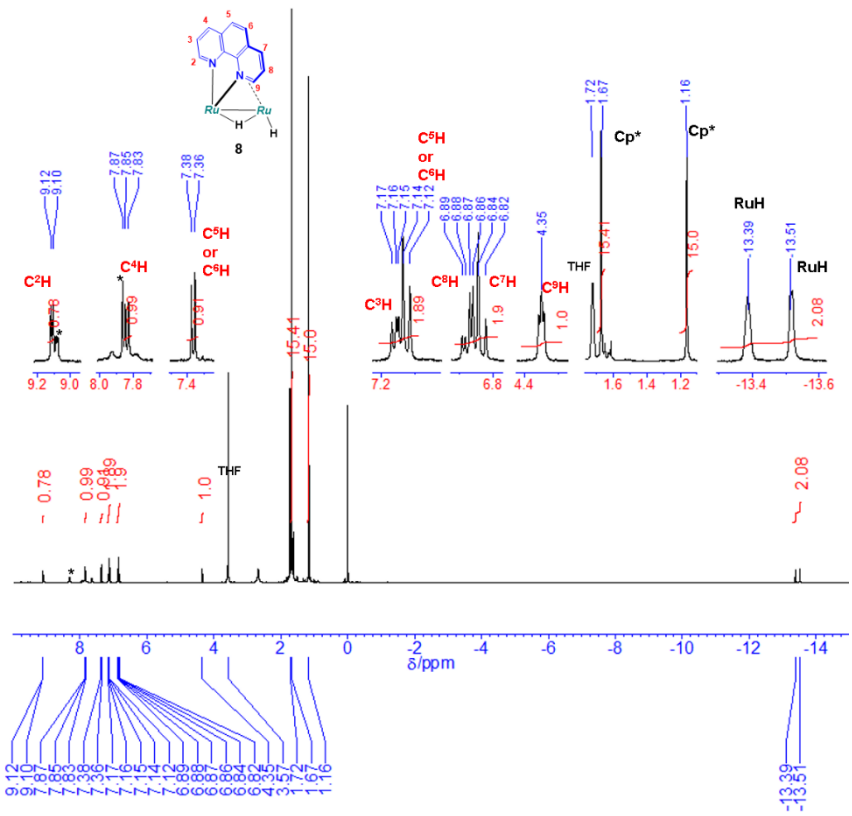

Figure S33. ^{1}H NMR spectrum of **8** (400 MHz, THF-d_8, –25 °C).

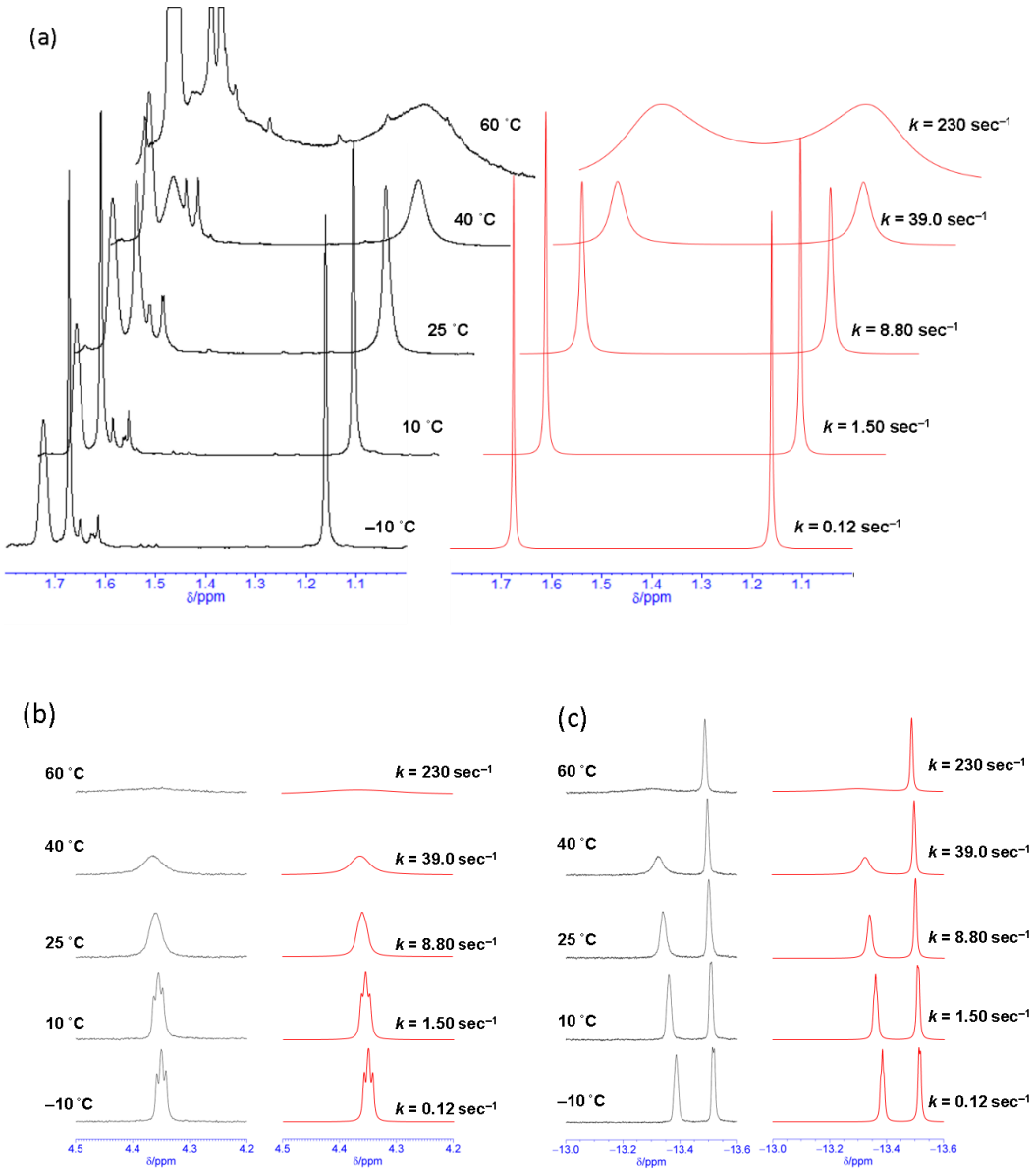

Figure S34. Variable temperature ^{1}H NMR spectra of **8** showing (a) Cp*, (b) methine, and (c) hydrido regions with simulated spectra (400 MHz, THF-d_8).

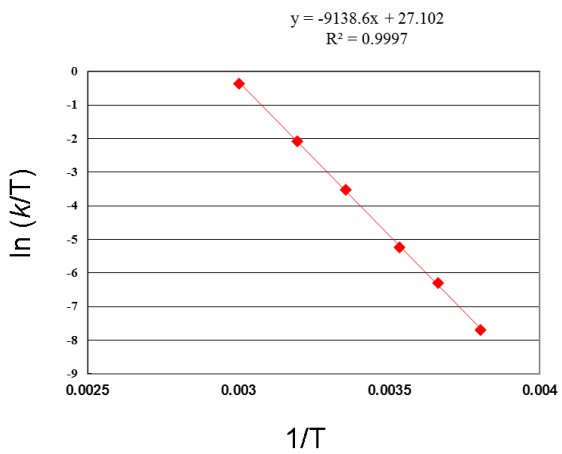

Figure S35. Eyring plot for the dynamic process of **8**.

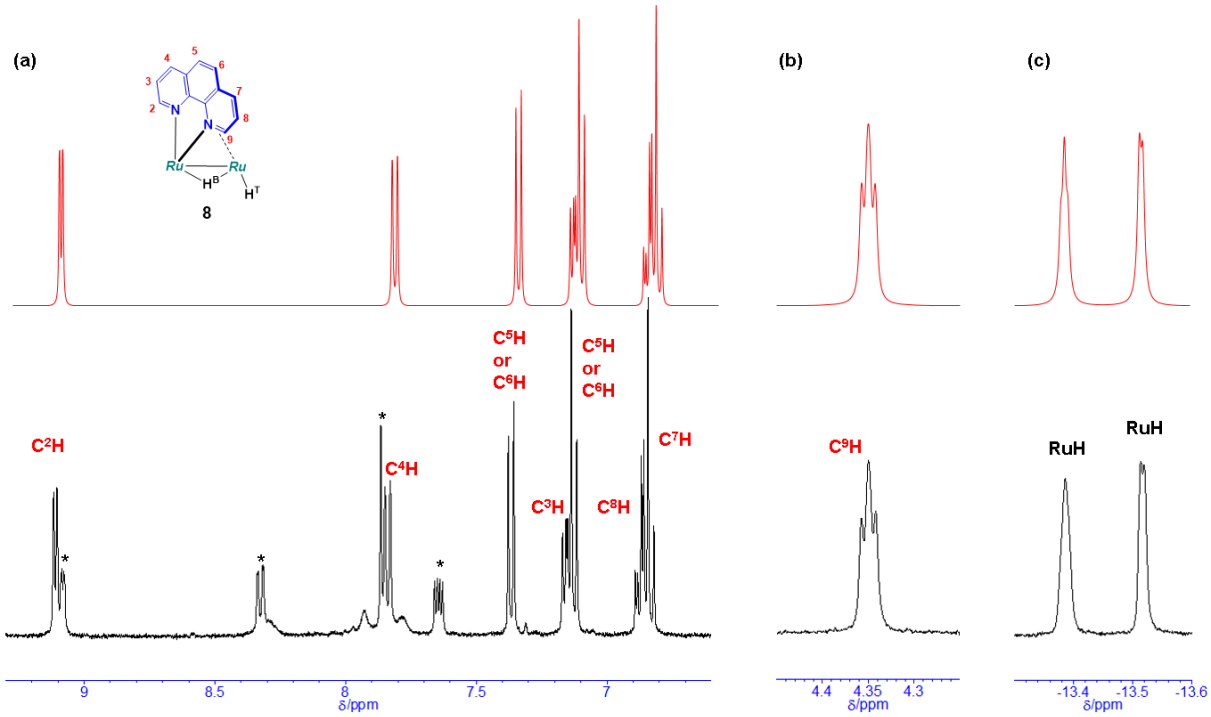

Figure S36. ^{1}H NMR spectra of **8** showing (a) phen, (b) methine, and (c) hydrido regions (black) and their simulated spectra (400 MHz, THF-d_8, –25 °C).Signals with an asterisk were derived from contaminated 1,10-phenanthroline.

Table S8. Estimated coupling parameters for the phenanthroline protons and hydrides of **8** at –25 °C.

		δ /ppm	W /Hz	*J*[1]	*J*[2]	*J*[3]	*J*[4]	*J*[5]	*J*[6]	*J*[7]	*J*[8]	*J*[9]
1	RuH	–13.516	2.30									
2	RuH	–13.385	2.40	2.00								
3	C^9H	4.350	1.80	0.50	2.50							
4	C^7H	6.835	1.70	0.00	0.00	0.10						
5	C^3H	7.154	1.90	0.00	0.00	0.00	0.00					
6	C^5H or C^6H	7.127	1.80	0.00	0.00	0.00	0.00	0.00				
7	C^8H	6.872	1.70	0.00	0.00	3.80	8.90	0.00	0.00			
8	C^5H or C^6H	7.367	1.270	0.00	0.00	0.00	0.00	0.00	8.20	0.00		
9	C^4H	7.839	1.80	0.00	0.00	0.00	0.00	7.96	0.00	0.00	0.00	
10	C^2H	9.111	1.70	0.00	0.00	0.00	0.00	4.94	0.00	0.00	0.00	1.05

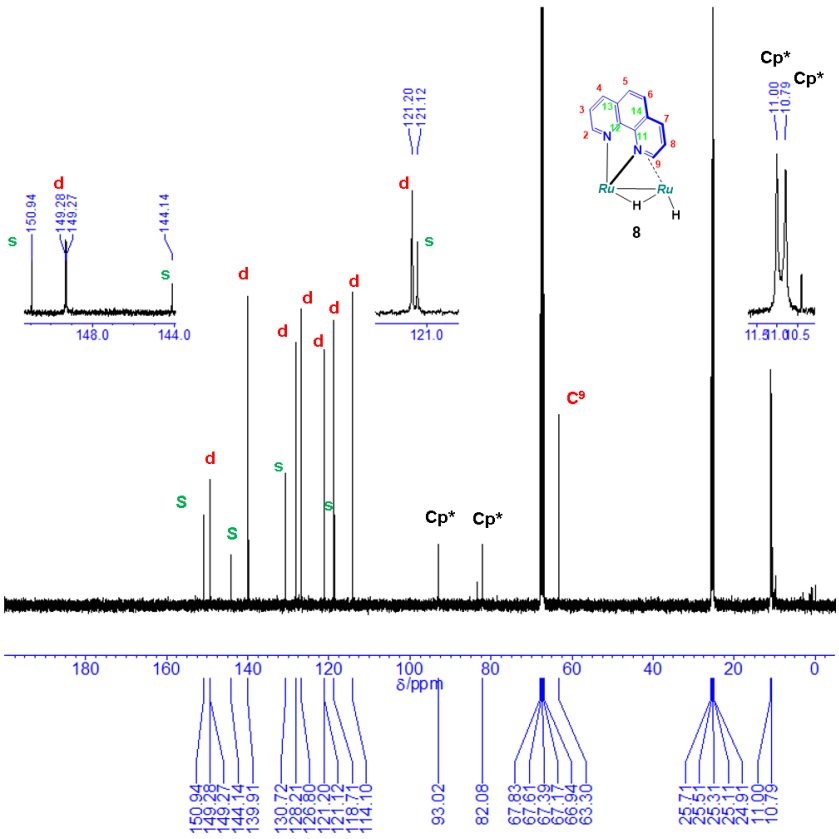

Figure S37. $^{13}C\{^{1}H\}$ NMR spectrum of **8** (100 MHz, THF-d_8, 25 °C).

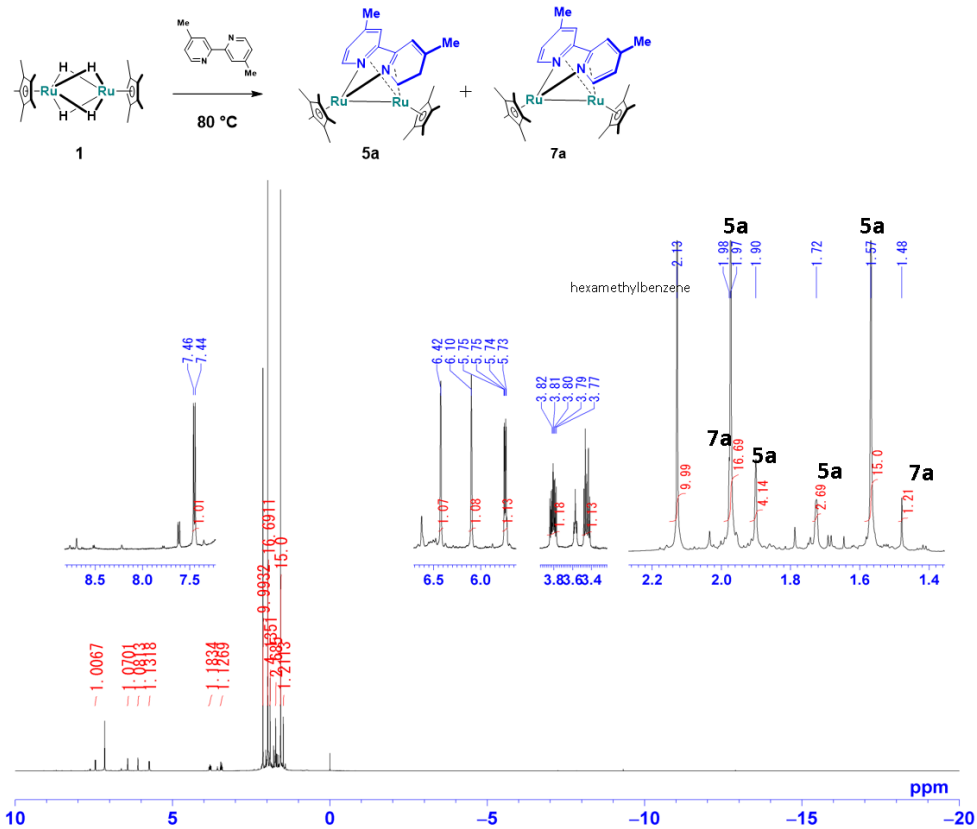

Figure S38. ^{1}H NMR spectrum of the mixture obtained by reaction of **1** with 4,4′-dimethyl-2,2′-bipyridine (400 MHz, C_6D_6, 25 °C).

3. Preliminary result of an X-ray diffraction study for 5a

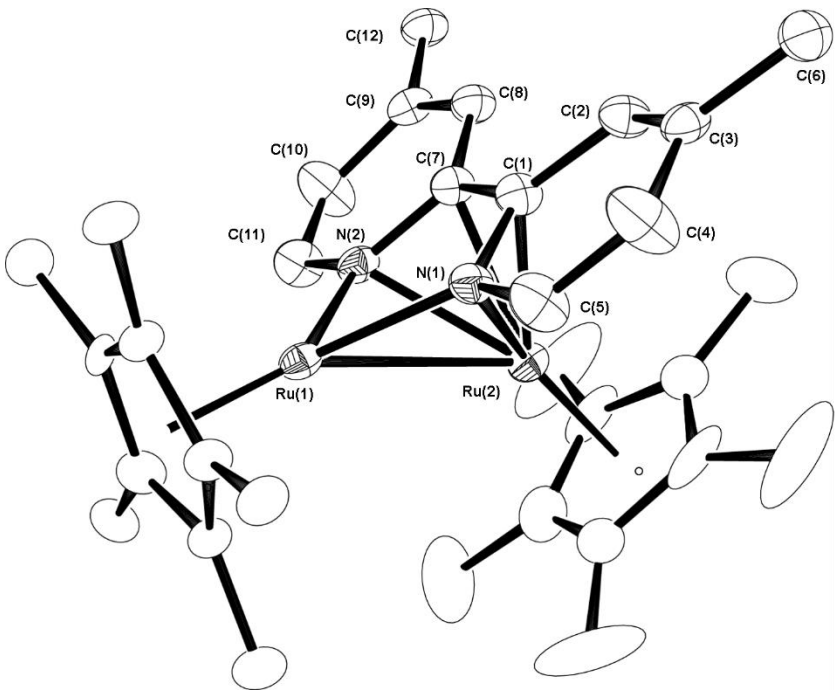

Figure S39. Molecular structure of **5a** (Preliminary result). Disorder in the dihydrobipyridine moiety could not be resolved (C(4), C(5), C(10), and C(11) atoms). Monoclinic, C_2/c, a = 21.7838(13) Å, b = 17.3872(11) Å, c = 16.5280(9) Å, β = 113.051(8)°, V = 5760.3(7) Å^3, Z = 8, Temp = 123 K, R (> 2σ) = 0.0774, wR_2 (> 2σ) = 0.1204. GOF =1.080.